

### **REMARKS**

Prior to this Amendment, claims 1-13 were pending in this application, of which claims 11 and 12 were withdrawn from consideration. By this Amendment, Applicants have amended claims 1, 6 and 10, cancelled claims 3, 4 and 9 without prejudice or disclaimer of the subject matter recited therein and added claims 32-52.

Applicants do not acquiesce in the Examiner's rejections, but instead have elected to make the above-mentioned amendments in an effort to expedite prosecution of this application leading to issuance of a patent. Reconsideration of the application as amended above and in view of the following remarks is earnestly solicited.

### **Claim Rejections**

#### **Priority**

In the Official Action, the Examiner notes that the instant application is a continuation-in-part ("CIP") of U.S. Patent Application Serial No. 10/610,068 (the '068 Application), which in turn claims the benefit of U.S. Patent Application Serial No. 60/442,644 (the '644 Application), filed on January 24, 2003. The Examiner further notes that the '068 Application is drawn to non-light activated composites and contends that the instant claims, which are directed to light-activated components, are not enabled by the '068 disclosure. Accordingly, the Examiner contends that the priority date of the '068 Application cannot be extended to the present application. However, Applicants respectfully disagree with the Examiner's assertion, particularly as the Examiner has failed to acknowledge that the present application directly claims the benefit of the '644 Application and incorporates its disclosure by reference (see page 1, lines 7-9 of the present application as originally filed). As the present application claims the benefit of the '644 Application, its effective filing date is in fact January 24, 2003 (i.e., the filing date of the '644 Application), and not January 15, 2004. Moreover, as the '644 Application clearly discloses light-activated components such as those instantly claimed (see the attached copy of the '644 Application), Applicants respectfully contend that this subject matter is enabled as of January 24, 2003. Acknowledgement by the Examiner of January 24, 2003 as the priority date for the instant application is respectfully requested.

#### **Claim Rejection under 35 U.S.C. § 102 - Riley et al.**

The Examiner rejected claims 1-6 and 8 under 35 U.S.C. § 102(b) as being anticipated by the literature article "Improved Laser-Assisted Vascular Tissue Fusion Using Light-Activated Surgical Adhesive in a Porcine Model" to Riley et al., *Biomed. Sci. Instrum.*, Vol. 37, pages 451-456, 2001 ("Riley"). However, Applicants respectfully submit that Riley does

not support the Examiner's rejection under § 102(b) in light of the amendments and arguments made in this response. The case law is clear on this point. For a claim to be anticipated under 35 U.S.C. § 102, each and every limitation of the claim must be disclosed in a single prior art reference. General Electric Co. v. Nintendo Co., 50 USPQ2d 1910, 1915 (Fed. Cir. 1999) (citing PPG Industries, Inc. v. Guardian Industries Corp., 37 USPQ2d 1618, 1624 (Fed. Cir. 1996)) ("to anticipate a claim, a reference must disclose every element of the challenged claims and enable one skilled in the art to make the anticipating subject matter."). More particularly, the Federal Circuit has held that the test for anticipation is "[t]hat which would literally infringe if later in time anticipates if earlier than the date of invention." Lewmar Marine, Inc. v. Barient, Inc., 827 F.2d 744, 3 USPQ2d 1776 (Fed. Cir. 1987), cert. denied, 484 U.S. 1007 (1988). Furthermore, as the Federal Circuit has noted, there can be no anticipation "unless all of the same elements are found in exactly the same situation and united in the same way...in a single prior art reference." Perkin-Elmer Corp. v. Computervision Corp., 732 F.2d 888, 894, 221 USPQ (BNA) 669, 673 (Fed. Cir. 1984), citing Kalman v. Kimberly-Clark Corp., 713 F.2d 760, 771, 218 USPQ (BNA) 781, 789 (Fed. Cir. 1983).

#### Independent Claims 1 and 6

Riley fails to meet the requirements needed to satisfy a *prima facie* case of anticipation under 35 U.S.C. § 102(b) by not disclosing "each and every" limitation of amended independent claims 1 and 6. More particularly, Riley is directed to light-activated adhesives composed of a poly(L-lactic-co-glycolic acid) scaffold and doped with a traditional protein solder mix of porcine serum albumin and indocyanine green dye (see generally, Riley's Abstract). However, Applicants find no teaching in Riley of light absorbers selected from at least one of red food coloring, blue food coloring and green food coloring nor light absorbers having a concentration of about 200 – 1000 µL / 13 mL of deionized water, as specifically required by amended independent claims 1 and 6, respectively. As such, Riley does not disclose each element of the claimed invention nor satisfy the anticipation standard under § 102, which specifically requires that all of the elements be found in "exactly the same situation and united in the same way" in a single prior art reference. Accordingly, the Examiner's rejection of amended independent claims 1 and 6 as being anticipated by Riley under § 102(b) should be withdrawn. Removal of the rejection and allowance of claims 1 and 6 is respectfully requested. If the Examiner should disagree with the Applicants' arguments, the Examiner is asked to kindly point out with particularity where these

limitations are expressly disclosed with the teachings of Riley.

Dependent Claims 2, 5 and 8

Claims 2, 5 and 8 each depend from one of independent claims 1 and 6. Since claims 1 and 6 are believed to be allowable for the reasons discussed above, claims 2, 5 and 8 are also believed to be allowable. Removal of the rejection and allowance of claims 2, 5 and 8 is respectfully requested. If the Examiner should disagree with the Applicants' arguments, the Examiner is asked to kindly point out with particularity where in the prior art the limitations of the dependent claims are expressly disclosed within Riley.

**Claim Rejection under 35 U.S.C. § 102 - McNally et al.**

The Examiner rejected claims 1-6 and 8 under 35 U.S.C. § 102(b) as being anticipated by the literature article "Improved Vascular Tissue Fusion Using New Light-Activated Surgical Adhesive on a Canine Model" to McNally et al., Journal of Biomedical Optics, vol. 6, no. 1, pp. 68-73, January 2001 ("McNally"). However, Applicants respectfully submit that McNally does not support the Examiner's rejection under § 102(b) in light of the amendments and arguments made in this response.

Independent Claims 1 and 6

McNally fails to meet the requirements needed to satisfy a *prima facie* case of anticipation under 35 U.S.C. § 102(b) by not disclosing "each and every" limitation of amended claims 1 and 6. More particularly, McNally is directed to a surgical adhesive composed of a poly(L-lactic-co-glycolic acid) scaffold and doped with a traditional protein solder mix of bovine serum albumin and indocyanine green dye (see generally, McNally's Abstract). However, Applicants find no teaching in McNally of light absorbers selected from at least one of red food coloring, blue food coloring and green food coloring nor light absorbers having a concentration of about 200 – 1000 µL / 13 mL of deionized water as specifically required by amended independent claims 1 and 6, respectively. As such, McNally does not disclose each element of the claimed invention nor satisfy the anticipation standard under § 102, which specifically requires that all of the elements be found in "exactly the same situation and united in the same way" in a single prior art reference. Accordingly, the Examiner's rejection of amended independent claims 1 and 6 as being anticipated by McNally under § 102(b) should be withdrawn. Removal of the rejection and allowance of claims 1 and 6 is respectfully requested. If the Examiner should disagree with the Applicants' arguments, the Examiner is asked to kindly point out with particularity where these limitations are expressly disclosed with the teachings of McNally.

Dependent Claims 2, 5 and 8

Claims 2, 5 and 8 each depend from one of independent claims 1 and 6. Since claims 1 and 6 are believed to be allowable for the reasons discussed above, claims 2, 5 and 8 are also believed to be allowable. Removal of the rejection and allowance of claims 2, 5 and 8 is respectfully requested. If the Examiner should disagree with the Applicants' arguments, the Examiner is asked to kindly point out with particularity where in the prior art the limitations of the dependent claims are expressly disclosed within McNally.

**Claim Rejection under 35 U.S.C. § 102 - Moser et al.**

The Examiner rejected claims 1-6, 8 and 9 under 35 U.S.C. § 102(b) as being anticipated by the literature article "New Range of Light-Activated Surgical Adhesives for Tissue Repair" to Moser et al., *Biomed. Sci. Instrum.*, Vol. 37, pages 441-449, 2001 ("Moser"). However, Applicants respectfully submit that Moser does not support the Examiner's rejection under § 102(b) in light of the amendments and arguments made in this response.

Independent Claims 1 and 6

Moser fails to meet the requirements needed to satisfy a *prima facie* case of anticipation under 35 U.S.C. § 102(b) by not disclosing "each and every" limitation of amended claims 1 and 6. More particularly, Moser is directed to a surgical adhesive composed of a poly(L-lactic-co-glycolic acid) scaffold and doped with a traditional protein solder mix of bovine serum albumin and a chromophoric dye, such as indocyanine green dye (see generally, Moser's Abstract). However, Applicants find no teaching in Moser of light absorbers selected from at least one of red food coloring, blue food coloring and green food coloring nor light absorbers including one of food colorings, pH indicators, water and hemoglobin and having a concentration of about 200 – 1000  $\mu\text{L}$  / 13 mL of deionized water as specifically required by amended independent claims 1 and 6, respectively. As such, Moser does not disclose each element of the claimed invention nor satisfy the anticipation standard under § 102, which specifically requires that all of the elements be found in "exactly the same situation and united in the same way" in a single prior art reference. Accordingly, the Examiner's rejection of amended independent claims 1 and 6 as being anticipated by Moser under § 102(b) should be withdrawn. Removal of the rejection and allowance of claims 1 and 6 is respectfully requested. If the Examiner should disagree with the Applicants' arguments, the Examiner is asked to kindly point out with particularity where these limitations are expressly disclosed with the teachings of Moser.

Dependent Claims 2, 5, 8 and 9

Claims 2, 5, 8 and 9 each depend from one of independent claims 1 and 6. Since claims 1 and 6 are believed to be allowable for the reasons discussed above, claims 2, 5, 8 and 9 are also believed to be allowable. Removal of the rejection and allowance of claims 2, 5, 8 and 9 is respectfully requested. If the Examiner should disagree with the Applicants' arguments, the Examiner is asked to kindly point out with particularity where in the prior art the limitations of the dependent claims are expressly disclosed within Moser.

**Claim Rejection under 35 U.S.C. § 102 - Hoffman.**

The Examiner rejected claims 1-10 and 13 under 35 U.S.C. § 102(a) as being anticipated by the literature article "Effect of varying chromophores used in light-activated protein solders on tensile strength and thermal damage profile of repairs" to Hoffman et al., *Biomed Sci Instrum.*, 39:12-17, 2003 ("Hoffman"). Responsive thereto, Applicants submit that Hoffman is not prior art. More particularly, as explained above, Applicants' effective filing date is January 24, 2003, i.e., the filing date of the '644 Application to which the instant application claims priority. Hoffman, on the other hand, has a publication date that is later than the instant application's filing date (i.e., April 2003) and therefore does not qualify as prior art. Applicants respectfully request that the Examiner withdraw this rejection.

**Claim Rejection under 35 U.S.C. § 103 – Moser**

The Examiner has rejected claim 10 under 35 U.S.C. § 103(a) as being unpatentable over Moser.

Claim 6, from which claim 10 depends, is discussed in detail above, as are the deficiencies of Moser with respect to claim 10. As Applicants find no teaching in Moser of light absorbers selected from at least one of red food coloring, blue food coloring and green food coloring nor light absorbers including one of food colorings, pH indicators, water and hemoglobin and having a concentration of about 200 – 1000  $\mu\text{L}$  / 13 mL of deionized water, one skilled in the relevant art would be unable to formulate the presently claimed compositions from the teachings of Moser. As such, it is submitted that the compositions defined by present claim 10 is nonobvious over and patently distinguishable from Moser, whereby the rejection under 35 U.S.C. § 103 has been overcome. Reconsideration is respectfully requested.

**New Claims**

New independent claim 48 further defines aspects of the disclosed compositions. Applicants submit that the prior art of record does not disclose, teach or suggest a light-

activated adhesive including a light absorber selected from at least one of red food coloring, blue food coloring and green food coloring and being selected to provide a solder/interface temperature of  $66 \pm 3^{\circ}\text{C}$ , as well as having a concentration of about 200 – 1000  $\mu\text{L}$  / 13 mL of deionized water, as recited in claim 48.

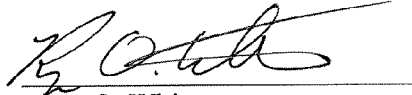
New dependent claims 32-47 and 49-52 recite additional features of the claimed compositions, which Applicants respectfully submit are not disclosed, taught or suggested by the prior art of record.

**Final Remarks**

Applicants submit that the application is now in condition for allowance and respectfully request that the same be granted. Applicants request that, if necessary, this Amendment be considered a request for an extension of time for a time appropriate for the amendment to be timely filed. Applicants request that any required fees for filing this Amendment be charged to the account of Bose McKinney & Evans LLP, Deposit Account Number 02-3223.

Respectfully submitted,

BOSE McKINNEY & EVANS

A handwritten signature in black ink, appearing to read 'R. O. White', is written over a horizontal line.

Ryan O. White

Registration No. 45,541

Indianapolis, Indiana  
(317) 684-5451

982988\_1

EL591988381US

Express Mail No. EL591988381US

PROVISIONAL PATENT APPLICATION

of

Karen M. McNally-Heintzelman,

Jeffrey N. Bloom,

Mark T. Duffy,

and

Douglas L. Heintzelman

For

IMPROVED LIGHT-ACTIVATED BIOLOGICAL ADHESIVES

Attorney Docket 12391-0016

## IMPROVED LIGHT-ACTIVATED BIOLOGICAL ADHESIVES

### BACKGROUND

The use of sutures is still the mainstay of most forms of modern-day surgery, whether internal surgery or external wound closure is involved. Inherent complications and drawbacks of suture use are numerous. Suture placement can be time-consuming. Sutures must be placed very precisely in order to properly align the tissue. Often the tissue must be manually realigned before each pass of the suture's needle. Imprecise placement of a suture may necessitate its removal and replacement; as a result, delicate tissues may be damaged. Sutures frequently must be removed postoperatively. Not only is this also time-consuming, but children often require either restraint, sedation, or additional exposure to general anesthetics. Sutures can also produce allergic reactions and act as a nidus for infection. Finally, sutures pose the risk of needle-stick injury and transmissible infections for operating room personnel.

The use of light-activated biological adhesives for tissue repair is known. For example, McNally et al., U.S. Patent No. 6,391,049, discloses the use of a biodegradable polymer scaffold in combination with a solder and a chromophoric dye for tissue repair and/or wound closure.

Improvements to light-activated surgical adhesives are desired, in order for such devices to be useful in a broad range of internal and external surgical and other medical applications.

### SUMMARY

One aspect of the present invention relates generally to novel combinations of light-activated biological adhesives with alternative chromophores. It has been discovered that readily-available food colorings may be used effectively as chromophores in combination with light-activated biological adhesives, and may provide additional beneficial features. It has also been discovered that pharmaceuticals that are capable of absorbing photons or electromagnetic radiation at specific wavelengths may also be used as alternative chromophores and could provide the additional advantage of drug delivery to a wound or repair site where appropriate.

Another aspect of the present invention relates to novel applications of light-activated biological adhesives. It has been discovered that light-activated biological adhesives may be used effectively in a broad range of internal and external surgical or other medical applications, including, but not limited to, certain ophthalmic surgical procedures.

Yet another aspect of the present invention relates to an improved scaffold-enhanced light-activated biological adhesive. It has been discovered that altering the scaffold pore size and/or surface irregularity impacts the effectiveness of the scaffold-enhanced light-activated adhesive.

**EXHIBITS**

The following Exhibits are attached hereto and incorporated herein by this reference:

Exhibit A – Jeffrey N. Bloom, M.D., Mark T. Duffy, M.D., Ph.D., Jason B. Davis, B.S., and Karen M. McNally-Heintzelman, Ph.D., *A Light-Activated Surgical Adhesive Technique for Sutureless Ophthalmic Surgery*;

Exhibit B – Jeffrey N. Bloom, M.D., Mark T. Duffy, M.D., Ph.D., Jason B. Davis, B.S., and Karen M. McNally-Heintzelman, Ph.D., *Light-Activated Surgical Adhesive: A Sutureless Alternative for Ophthalmic Surgery* (Abstract);

Exhibit C – Jeffrey N. Bloom, M.D., Mark T. Duffy, M.D., Ph.D., Jason B. Davis, B.S., and Karen M. McNally-Heintzelman, Ph.D., *Light-Activated Surgical Adhesive: A Sutureless Alternative for Ophthalmic Surgery* (Poster);

Exhibit D – Brian D. Byrd, M.S., Douglas L. Heintzelman, M.S., M.D., and Karen M. McNally-Heintzelman, Ph.D., *Alternative Chromophores for Use in Light-Activated Surgical Adhesives*;

Exhibit E – Grant T. Hoffman, Brian D. Byrd, M.S., Eric C. Soller, Douglas L. Heintzelman, M.S., M.D., and Karen M. McNally-Heintzelman, Ph.D., *Alternative Chromophores for Use in Light-Activated Surgical Adhesives: Optimization of Parameters for Tensile Strength and Thermal Damage Profile*;

Exhibit F – Additional photographs of one embodiment of the scaffold disclosed herein;

Exhibit G – Data relating to comparison of scaffolds having different pore sizes; and

Exhibit H – Data relating to comparison of results using scaffold with smooth surface to results using scaffold with irregular surface.

**BRIEF DESCRIPTION OF THE DRAWINGS**

Fig. 1 is a photograph of an embodiment of a scaffold suitable for use in a scaffold-enhanced light-activated biological adhesive, showing a first side of the scaffold;

Fig. 2 is a photograph of the scaffold of Fig. 1, showing a second side of the scaffold;

Fig. 3 is a photograph of the scaffold of Fig. 1, showing a first perspective view of the scaffold;

Fig. 4 is a photograph of the scaffold of Fig. 1, showing a second perspective view of the scaffold; and

Fig. 5 is a photograph of the scaffold of Fig. 1, showing a third perspective view of the scaffold.

### DETAILED DESCRIPTION

Chromophores are used in laser-tissue soldering to enhance the amount of light energy or radiation that is absorbed by the solder. However, the safety of the degradation products of commonly-used chromophores such as indocyanine green (ICG) and methylene blue following irradiation is uncertain. Also, many chromophores that absorb light in the visible range will decay with continued exposure to light. It has been found that red, green, and blue food colorings may be used effectively as chromophoric dyes in tissue soldering and have improved degradation characteristics over the commonly-used ICG. Exhibits D and E explain in detail the initial studies that have been conducted to evaluate the performance of these alternative chromophores in light-activated surgical adhesives.

Another alternative chromophore is a pH indicator, such as phenothaline red. Such a pH indicator may be incorporated into the solder material. If the solder material is kept at a pH that does not cause the pH indicator to turn color, the indicator will not absorb light and decay. A small amount of dilute acid or base can be added when the solder material is ready for use, causing the indicator to change color and thus assist in specific laser activation.

Yet another alternative chromophore is a pharmaceutical drug that absorbs electromagnetic radiation. It is presently contemplated that any drug or medication that absorbs photons, radiation having a wavelength in the electromagnetic spectrum (including, but not limited to, ultraviolet, visible, or infrared radiation) may be suitable for use as a chromophore in combination with a light-activated adhesive. For example, a commercially-available drug such as estradiol, which absorbs light in a wavelength approximately 400nm, may be used. Other possible pharmaceutical alternatives include rifampins, lycopenes, and phenazopyridine. Such drug chromophores offer the additional therapeutic advantage of providing medication to a wound or repair site.

It is contemplated that any of the above-mentioned novel combinations of light-activated

biological adhesive and alternative chromophores may be used alone. For example, during surgery, there are situations where physicians will use a light-activated adhesive by itself, such as in plastic surgery involving a face lift or large flap enhancement; or in other surgeries where a deep wound is closed in layers. See Exhibit D.

It is also contemplated that the above-mentioned novel combinations may also be used in combination with a scaffold, such as a biodegradable polymer scaffold. See Exhibit E.

Further, it has been discovered that light-activated adhesives may be used in a wide range of applications, including internal surgeries, external wound closures, and certain ophthalmic surgeries. For example, Exhibits A-C describe studies that have been conducted to evaluate the performance of a scaffold-enhanced light-activated solder in ophthalmic applications. The particular specifications of a scaffold-enhanced solder may be selected, for example, to maximize tensile strength, as discussed in further detail in Exhibits A-C. Yet further, it has been found that scaffold pore size and the nature of the scaffold surface (e.g., whether it is smooth or rough) may be varied to optimize tensile strength, consistency of repairs, or other parameters. This aspect of the invention is discussed in Exhibits G and H.

Figs. 1-5 show photographs of various views of one embodiment of a scaffold suitable for use in the scaffold-enhanced light-activated adhesive discussed above. In the illustrated embodiment, the scaffold has a circular shape. Fig. 1 shows that at least one side of the scaffold may have an irregular surface. Figs. 2 and 3 show that another side of the scaffold may have a substantially smooth surface. Additionally, Fig. 3 shows that the scaffold may take the form of a thin wafer. Figs. 4 and 5 show that the scaffold may be bent, folded, cuffed, or rolled to adapt to various applications. Additional photographs of the illustrated scaffold are provided in Exhibit G. As discussed above, it is understood that different embodiments of the scaffold may take a variety of forms and/or shapes.

Additional details, examples, and illustrations regarding the device, methods, and system

of the present invention and anticipated uses and benefits thereof, are set forth in the accompanying Exhibits. Although specific illustrated embodiments of the invention have been disclosed, it is understood by those of skill in the art that changes in form and details may be made without departing from the spirit and scope of the invention. The present invention is not limited to the specific details disclosed therein.

441159\_5

60442644.012403

12391-0016

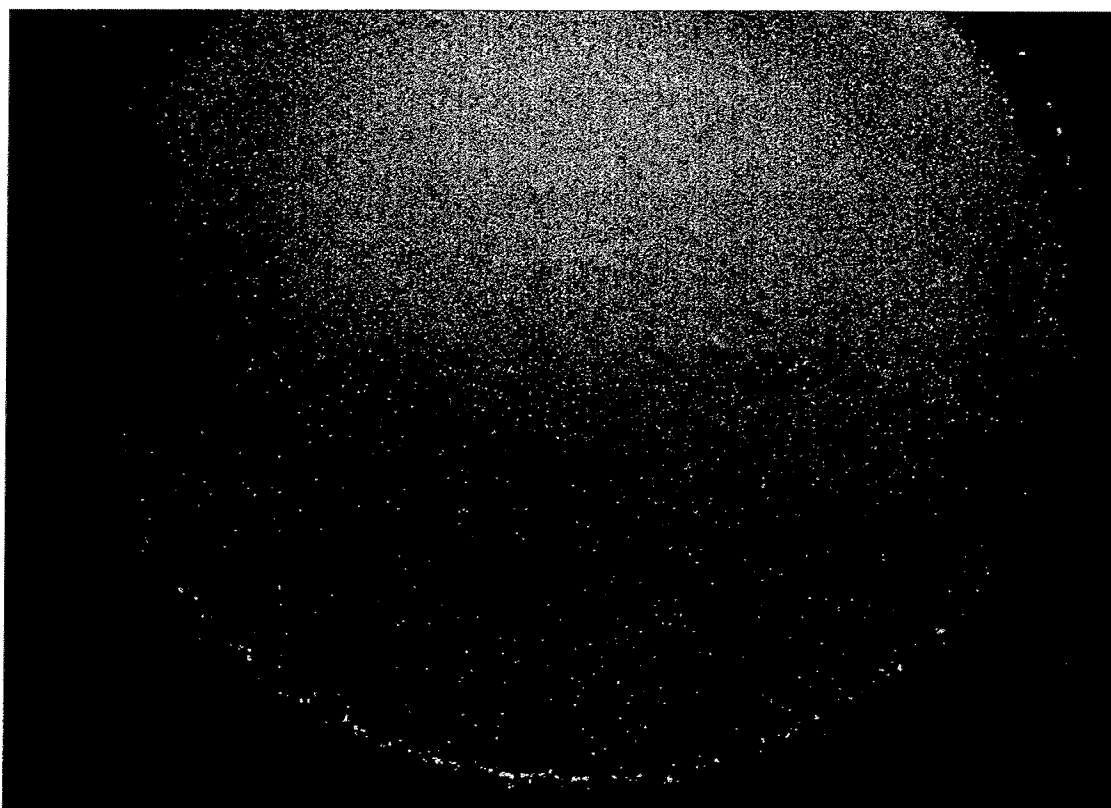


FIG. 1



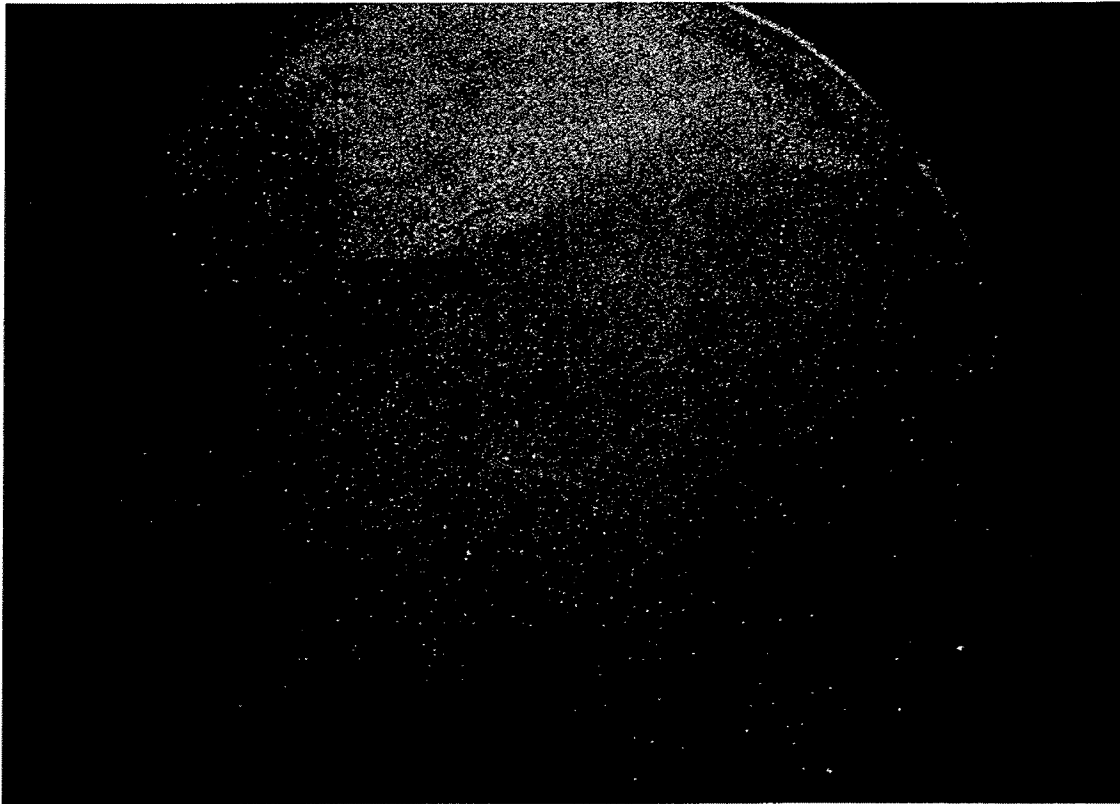


FIG. 2



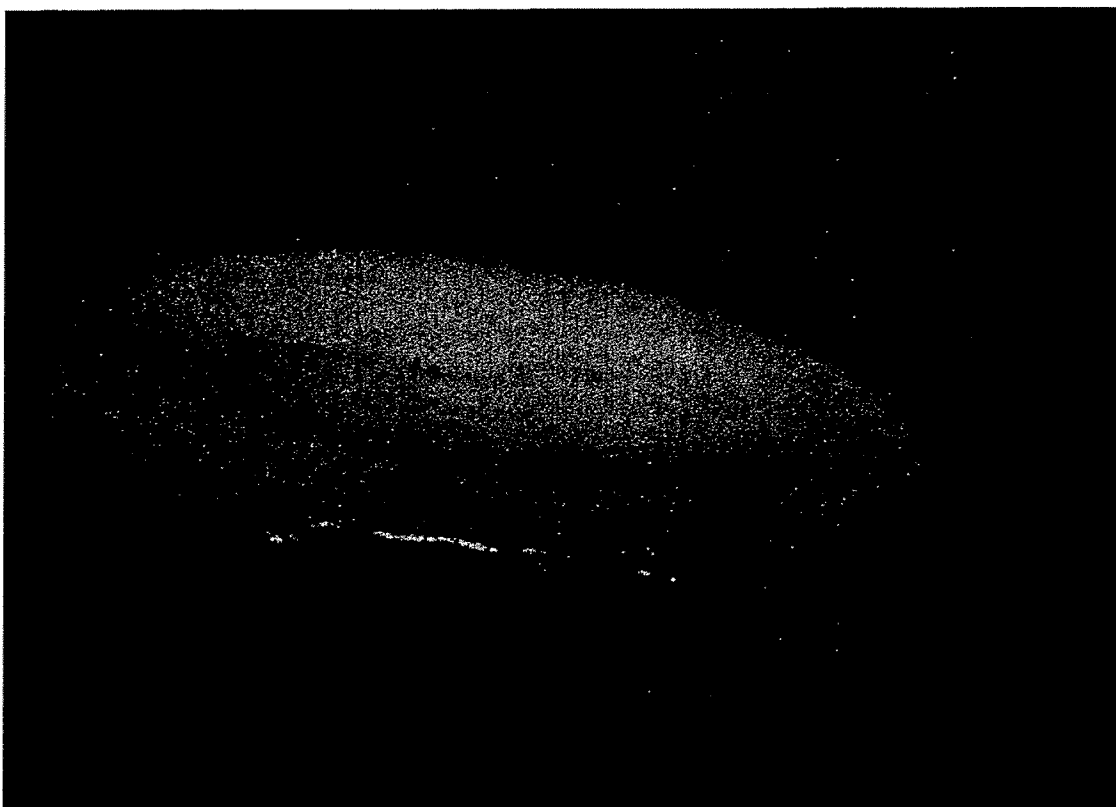


FIG. 3

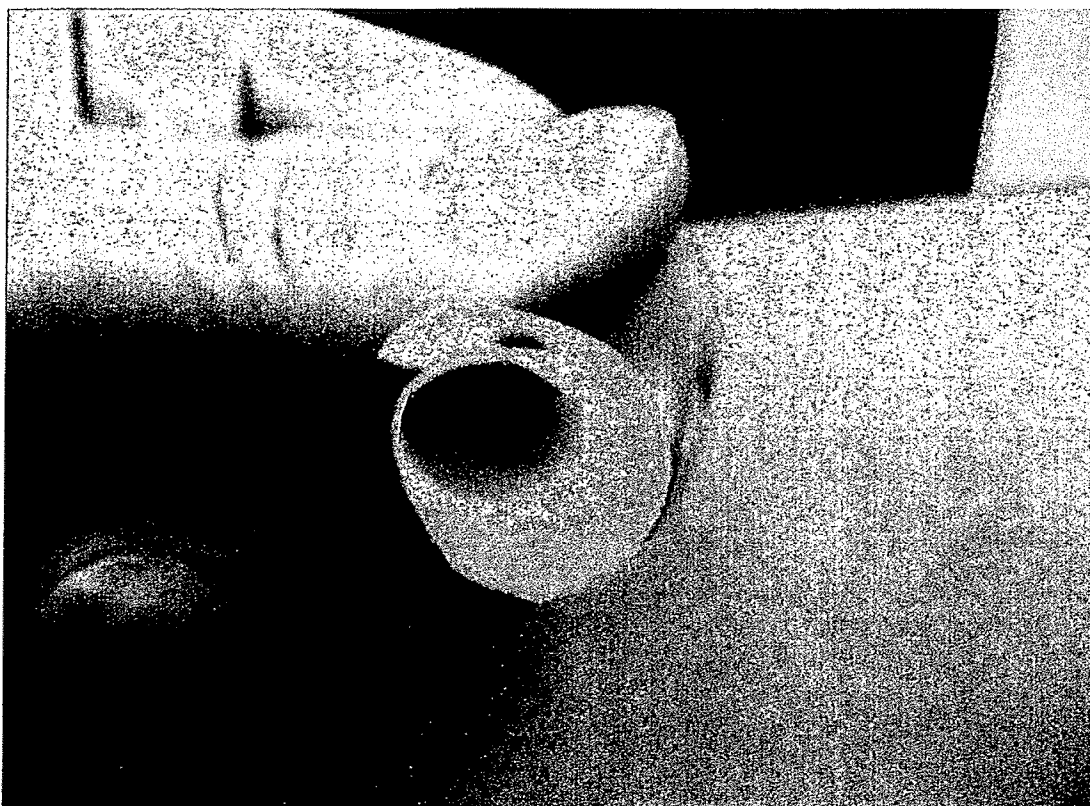


FIG. 4

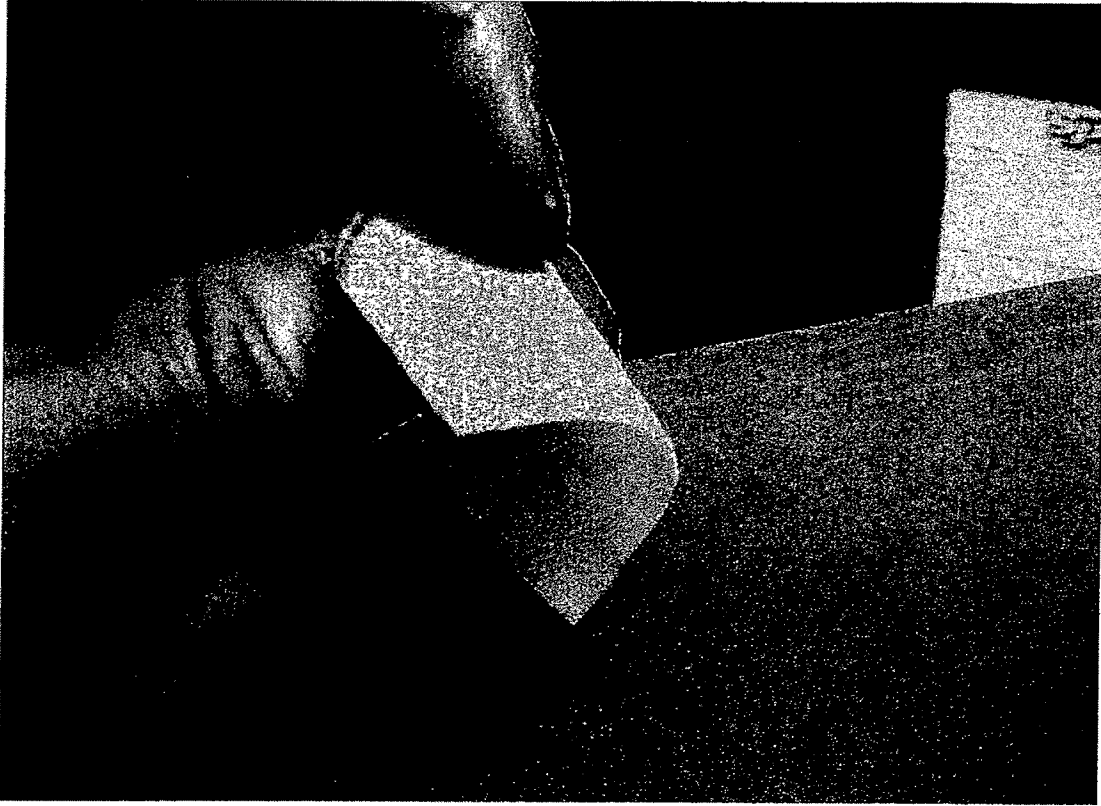


FIG. 5

**A Light-Activated Surgical Adhesive Technique  
For Sutureless Ophthalmic Surgery**

Jeffrey N. Bloom, MD<sup>1</sup>

Mark T. Duffy, MD, PhD<sup>1</sup>

Jason B. Davis, BS<sup>2</sup>

Karen M. McNally-Heintzelman, PhD<sup>2</sup>

<sup>1</sup>Department of Ophthalmology and Visual Sciences

University Of Illinois College Of Medicine

Chicago, Illinois

<sup>2</sup>Department of Applied Biology and Biomedical Engineering

Rose-Hulman Institute of Technology

Terre-Haute, Indiana

Correspondence / Reprints:

Jeffrey N. Bloom, MD

Department of Ophthalmology and Visual Sciences

University Of Illinois College Of Medicine

1855 W Taylor Street

Chicago, Illinois 60612

Phone: 312 – 996 - 7445      FAX: 312 – 945 – 1400

E-Mail: [jbloom@uic.edu](mailto:jbloom@uic.edu)

**OBJECTIVES:** We investigated a scaffold-enhanced light-activated bioadhesive technique as a substitute for sutures in ophthalmic surgery.

**CLINICAL RELEVANCE:** Suture use in ophthalmic surgery is technically-demanding, time-consuming and may be associated with serious complications, such as inadvertent ocular penetration which can result in retinal detachment and endophthalmitis.

Bioadhesive surgery could eliminate many complications and limitations associated with the use of sutures.

**METHODS:** The bioadhesive was composed of a poly(L-lactic-co-glycolic acid) (PLGA) porous scaffold doped with a protein solder mix composed of serum albumin and indocyanine green (ICG), which was activated with a diode laser. Extraocular muscle-to-muscle, sclera-to-sclera and extraocular muscle-to-sclera adhesions were created in freshly-harvested tissue followed by tensile strength testing of these surgical adhesions.

**RESULTS:** Optimum tensile strength for muscle-to-muscle repair was achieved with 50% w/v BSA and 0.5mg/ml of ICG saturated into a PLGA porous scaffold and activated with an 805nm diode laser. Tensile strength was 81% of native muscle tensile strength ( $433 \pm 70$  g vs.  $494 \pm 73$  g). Sclera-to-sclera adhesions achieved a breaking load of  $295 \pm 38$ g, while rectus muscle-to-sclera was  $309 \pm 37$  g.

**CONCLUSIONS:** Sutureless ophthalmic surgery utilizing this bioadhesive technique is feasible, technically simple and may result in reduced surgical complications and cost.

## INTRODUCTION

The use of sutures is the mainstay of most forms of modern-day surgery. Until very recently, virtually all ophthalmic surgery was only possible with specialized sutures and needles. Strabismus correction, corneal transplantation, vitreoretinal surgery, trauma repair, oculoplastic procedures, glaucoma surgery, and extracapsular cataract removal all require precise suture placement through various fine structures of the eye and adnexa. While microscopes, loupe magnification and specialized illumination techniques have made it easier to perform ophthalmic surgery, suture placement is technically difficult, time-consuming and may be associated with serious complications.

For example, strabismus surgery requires that a suture be inserted and advanced within the sclera at a depth of approximately half the scleral thickness. This is usually performed with the aid of loupe magnification. Perforation of the sclera during reattachment of an extraocular muscle may be associated with the vision-threatening complications of retinal detachment and endophthalmitis.<sup>1,2</sup> It has also recently been suggested that contaminated intrascleral sutures may produce endophthalmitis even in the absence of scleral perforation.<sup>3,4</sup> Suture use in corneal transplantation may be associated with postoperative astigmatism and wound leakage.<sup>5</sup> Traumatic stellate corneal lacerations can be difficult to close using sutures due to their complex, irregular geometry, while posterior scleral sutures required in the repair of a ruptured globe may be arduous to insert without putting excessive pressure on the eye.

Inherent complications and drawbacks of suture use are numerous. Suture placement can be time-consuming. Sutures must be placed very precisely in order to properly align the tissue. Often the tissue must be manually realigned before each pass of

the suture's needle. Imprecise placement of a suture may necessitate its removal and replacement; as a result, delicate ocular tissues may be damaged. Sutures frequently must be removed postoperatively. Not only is this time-consuming, but children often require either restraint, sedation, or additional exposure to general anesthetics. Sutures can also produce allergic reactions and act as a nidus for infection. Finally, sutures pose the risk of needle-stick injury and transmissible infections for operating room personnel.

Currently, the only sutureless ophthalmic procedure is small-incision phacoemulsification of cataractous lenses. Attempts at utilizing bioadhesives in ophthalmic surgery have been limited. At present, the only bioadhesives used in clinical ophthalmic procedures are cyanoacrylates for corneal perforations.<sup>6,7</sup> Fibrin glue has been used for experimental strabismus surgery in rabbits, but its tensile strength has been disappointing.<sup>8,9</sup> 2-octyl-cyanoacrylate glue has also been used for rabbit strabismus surgery,<sup>10</sup> as well as attaching rabbit extraocular muscles to porous anophthalmic implants,<sup>11</sup> and has demonstrated greater adhesive strength. However, liquid adhesives may be difficult to precisely position on the sclera and the rapid hardening time after placement requires quick and accurate placement of the muscle. Cyanoacrylate glue has also proven to be of limited efficacy in the repair of leaking filtering blebs.<sup>12</sup>

We now report the use of a porous poly(L-lactic-co-glycolic acid) (PLGA) scaffold combined with a light-activated serum albumin solder as a substitute for sutures in ophthalmic surgery. This technique was utilized for *ex vivo* experiments in which fresh tissues were reattached -- extraocular muscle-to-extraocular muscle, sclera-to-sclera, and extraocular muscle-to-sclera -- and tensile strength of these bonds was tested following reattachment.

## MATERIALS & METHODS

### Experimental Groups

All experiments were designed and carried out with appropriate institutional IRB and Animal Care Committee approval. Three experimental groups were investigated: bonding of (I) extraocular rectus muscle-to-rectus muscle (four subgroups with n=10 each), (II) sclera-to-sclera (n=20), and (III) extraocular rectus muscle-to-sclera (n=20). In the first experimental group, rabbit superior rectus muscles were harvested approximately 45 minutes after sacrificing the animals. Tissue specimens were stored in phosphate buffered saline for a maximum of four hours at 4 °C before they were prepared for experiments. In the second group, eye bank human sclera was obtained and stored in phosphate buffered saline for a maximum of two days at 4 °C prior to use. In the third group, porcine orbits were obtained from a slaughterhouse approximately 4 hours after sacrificing the animals and stored in phosphate buffered saline for a maximum of two days at 4 °C before being utilized.

### Preparation of the Surgical Adhesive

Porous synthetic polymer scaffolds were prepared from PLGA, with a lactic:glycolic acid ratio of 85:15, using a solvent casting and particulate leaching technique.<sup>13</sup> The scaffolds were cast by dissolving 200mg PLGA in 2ml dichloromethane. Sodium chloride (salt particle size:  $\leq 106\mu\text{m}$  or 106-150 $\mu\text{m}$ ) with a 70% weight fraction was added to the polymer mix. The polymer solution was then cast in a 60mm Petri dish and left in a fume hood for 24 hours to allow the dichloromethane to evaporate. The salt was leached out of the polymer scaffolds, by immersion in filtered deionized water for 24

hours, to create the porous scaffolds. During this period the water was changed 3-4 times at approximately 8 hour intervals. The scaffolds were then air-dried and stored at room temperature until required.

Protein solder was prepared from either 25%(w/v) or 50%(w/v) bovine serum albumin (BSA) (Cohn Fraction V) and Indocyanine Green (ICG) dye at a concentration of 0.5 mg/ml, mixed in deionized water. The compounds were used without further purification. The solder was stored in lightproof plastic vials at 4 °C until required. Solder not used within one week was discarded.

The PLGA scaffolds were cut into rectangular pieces with the desired dimensions. The scaffolds were left to soak for a minimum of two hours in the protein solder mix before use. The thickness of the solder-doped polymer scaffolds, determined by scanning electron microscopy and measurement with precision calipers, was in the range of 200 to 205  $\mu\text{m}$ .

### **Tissue Repair Procedure**

Group I: The length and thickness of each muscle specimen was  $8.0 \pm 2.0$  mm and  $1.5 \pm 0.1$  mm, respectively. A complete transection (n=40) was accomplished with a #15 Bard-Parker blade and opposing ends were placed together on a piece of parafilm. Four sets of adhesive fabrication parameters were studied. Each parameter set differed in protein concentration and scaffold porosity (Table 1). Before depositing the adhesive, the tissue surface was blotted with cotton gauze to remove excess moisture. A strip of adhesive with surface dimensions of  $3.0 \times 1.0$  mm was then placed over the transection and irradiated with a diode laser operating at a wavelength of 805 nm (Opto Power Corp.,

Tucson, AZ). The laser light was coupled into a 660 $\mu$ m diameter silica fiber bundle and focused onto the adhesive surface with an imaging hand-piece connected at the end of the fiber. Since 805 nm is outside the visible spectrum, the laser includes a low-power aiming beam at 632 nm to assist the operator. Surgical outcome is unaffected by the aiming beam due to its low irradiance, as well as the poor absorption of the chromophore at this wavelength. The diode was operated in continuous mode with a spot size at the adhesive surface of approximately 1 mm. An irradiance of 15.9 W/cm<sup>2</sup>, as measured using a Fieldmaster GS power meter with a LM100 thermopile detector (Coherent Scientific, Santa Clara, CA), was used to denature the adhesive, with a scan rate of approximately 0.5 mm/s. Breaking point tensile strength was measured within minutes of solder activation.

Group II: Sclera tissue specimens (n=20) with surface dimensions of 4.0  $\times$  3.0 mm were prepared. A full thickness incision was cut through the tissue specimen width using a scalpel and opposing ends were placed together. The same repair procedure used for Group I was applied, with the exception that only the optimal adhesive parameters determined in Group I were tested (set D). Tensile strength was measured within minutes of solder activation.

Group III: A 360° conjunctival peritomy was performed on the globes exposing the sites of extraocular muscle attachment. The superior rectus muscle was carefully dissected from the globe using scissors. With the use of sharp dissection, all other attachments to the globe were then removed. The rectus muscle was re-approximated to the sclera using a pair of forceps such that the end of the muscle was located adjacent to, but not overlying the original site of insertion. A piece of adhesive with surface

dimensions of  $3.0 \times 1.0$  mm was then applied across the top of the tissues in a band-aid-like fashion and irradiated with the laser. The point of attachment was thus the superior aspect of the muscle. As with Group II, the same repair procedure used for Group I was applied, with the exception that only the optimal adhesive parameters determined in Group I were tested (set D). Tensile strength was measured within minutes of solder activation.

### **Tensile Strength Analysis**

Tensile strength analysis of the repairs was performed using a calibrated MTS Material Strength Testing Machine (858 Table Top System, MTS, Eden Prairie, MN), interfaced with a computer. The repaired tissue specimens were clamped to the tensiometer by pneumatic grips attached to a 500N load cell and pulled apart at a rate of 1 gravitational force per second until the repair failed. Failure was defined as complete separation of the tissue edges. The maximal load in grams was recorded at the breaking point. The tissue specimens were kept moist during this procedure to avoid the false elevations of repair strength associated with drying.<sup>14</sup> A two-way analysis of variance (ANOVA) was used to analyze and test for mean differences in tensile strength due to BSA and pore size, as well as testing for eventual interaction between these two factors.

## RESULTS

### Extraocular Rectus Muscle-Muscle Adhesion (Table 2)

Rabbit rectus muscle-to-muscle scaffold soldering was performed to optimize parameters for more physiologic surgical simulations. Four groups were tested (Table 1) in a two-factor two-level experimental design. Group I utilized a 25% w/v albumin solder with a scaffold pore size  $<106\mu\text{m}$ . Group II had 25% w/v albumin with a scaffold pore size of  $106\text{--}150\mu\text{m}$ . Group III had 50% w/v albumin solder with a scaffold pore size  $<106\mu\text{m}$  and Group IV had 50% w/v albumin with a scaffold pore size of  $106\text{--}150\mu\text{m}$ . Rabbit extraocular muscle had an intrinsic breaking load of  $494 \pm 73$  g. This was the peak tension carried by the muscle before failing. ANOVA statistical analysis demonstrated that tensile strength was significantly greater at the higher level of BSA concentration and pore size without significant interaction between these variables. A 50% w/v BSA mixture with 0.5mg/ml of ICG and a PLGA scaffold with pore size from  $106\text{--}150\mu\text{m}$  produced the greatest tensile strength (Table 2). This provided a breaking load of  $433 \pm 70$  g or 88% of inherent tissue strength.

### Sclera-to-Sclera Adhesion (Table 3)

Utilizing a 50% w/v BSA solder with 0.5mg/ml ICG in a PLGA scaffold ( $106\text{--}150\mu\text{m}$  pore size) uniform  $4.0 \times 3.0$  mm pieces of human sclera were joined together. Two pieces were positioned adjacent to each other on a piece of parafilm. Scaffolds impregnated with solder were trimmed to a size of  $3.0 \times 1.0$  mm, placed across the two pieces in a bridging fashion, and denatured with the 805nm diode laser. Tensile strengths were then

measured within minutes of adhesion. Table 3 shows the distribution of tensile strengths of these sutureless sclera-to-sclera bonds. The average breaking load was  $295 \pm 38$  g.

#### Extraocular Rectus Muscle-to-Sclera Adhesion (Table 4)

Fresh porcine rectus muscles were surgically removed from sclera. The rectus muscles were then placed on an adjacent area of bare sclera away from the original site of insertion. Excess moisture was blotted away. The  $3.0 \times 1.0$  mm polymer scaffold saturated with solder was placed across the top of the muscle bridging onto the sclera anterior to the muscle and denatured using an 805nm diode laser. Tensile strength was tested within minutes. Table 4 lists the range of breaking strengths of the resulting repairs. The mean tensile strength of the sutureless bond was  $309 \pm 37$  g.

The analysis of variance indicated a strong effect of BSA in the mean tensile strength ( $P=0.001$ ), as well as a strong effect of pore size ( $P<0.001$ ). In addition, no statistically significant interaction between these factors was found ( $P=0.793$ ).

## DISCUSSION

In all surgical specialties, suture placement requires precision and skill. In ophthalmic surgical procedures, suture placement and securing is time-consuming and technically demanding, even for the most experienced surgeon, because of the delicate nature of the eye tissue and the correspondingly small size of the suture and needle. Serious complications such as ocular penetration may cause endophthalmitis or retinal detachment. The manipulation of fine needles may also place operating room personnel and physicians at risk for needle-stick injuries and transmission of serious diseases. Many surgical specialties have substituted bioadhesives to replace or aid suture techniques in various procedures, including vascular surgery, skin closure (particularly in pediatric cases), and orthopedic procedures.<sup>15-19</sup>

The evolution of laser tissue soldering has occurred over the past 15 years. Laser tissue soldering is a bonding technique in which protein solder is applied to the tissue surfaces to be joined and laser energy is used to bond the solder to the tissue surfaces. The efficacy of diode laser tissue soldering using ICG-doped albumin protein solders has been demonstrated in a wide range of tissues, including blood vessels, genitourinary tract, gastrointestinal tract, liver, nerves, dura mater, skin, trachea and cartilage, with promising results.<sup>20,21</sup> Recent success has been demonstrated with a new light-activated surgical adhesive used to achieve vascular anastomoses.<sup>22,23</sup> This surgical adhesive is composed of a polymer scaffold doped with serum albumin and a chromophoric dye. PLGA, a copolymer of glycolic acid and lactic acid, is degraded *in vivo* by hydrolysis of the ester bonds. The products are eliminated through normal metabolic pathways.<sup>24</sup> In addition to current usage in biodegradable sutures, these materials have been evaluated as potential

drug delivery systems. The *in vivo* degradation rate, and consequently the drug delivery rate, can be modified by altering the composition of the polymer.<sup>24,25</sup> Thin films of PLGA of various thickness are easily fabricated in the laboratory using a solvent casting technique. When doped with serum albumin, the scaffolds provide better flexibility, as well as improved repair strength, over previous published results using albumin protein solders alone.<sup>26</sup> The chromophoric dye, ICG, provides for selective absorption of the laser irradiation. The end-result is a new surgical adhesive, which can be light-activated and used to join tissues together.

In the above reported experiments, a scaffold-enhanced light-activated protein solder was used to replace sutures in ocular tissues commonly joined by suturing. The breaking point of the extraocular muscle-to-sclera bond utilizing our repair technique was beyond that of the actively developed horizontal fixation force measured *in vivo* in humans and suggests that this procedure may be applicable for eye muscle surgery.<sup>27</sup> The authors of this previous study found a mean active fixation force at 50 degrees extreme gaze of 74.8 g for the medial rectus muscle and 59.1 g for the lateral rectus muscle, with a range of 48 to 103 g for all individuals measured, much less than that created by the scaffold-enhanced light-activated protein solder bond.

An ideal bioadhesive should have several critical properties. It must possess sufficient tensile strength to maintain wound integrity until the healing processes have restored sufficient tensile strength to resist failure under normal circumstances. It must be easily applied in a precisely controlled fashion. Non-viscous liquids are difficult to control and spread beyond the desired area of application. Excessively viscous adhesives may be difficult to uniformly apply or denature evenly throughout the entire area of

application. The ideal adhesive must “set” quickly, but only when desired. Although newer cyanoacrylates are strong and produce little inflammation, they have the disadvantage of difficult application and rapid hardening before the tissues can be properly aligned. Light-activated solders are ideal in that activation is rapid, controlled and limited to the area of precise absorption of the laser irradiation. Our repair technique is advantageous in that the solder remains contained in a porous scaffold. The scaffold can be made in any shape or size and custom-cut if desired. This facilitates alignment, quick and precise solder activation, and enhanced tensile strength. In addition, the scaffold can conceivably act as a temporary reservoir for the release of drugs, such as steroids, antibiotics, growth factors or growth factor inhibitors.<sup>28</sup> Finally, an ideal adhesive must be nontoxic, available in sterile preparation and not produce excessive inflammation beyond that occurring in secondary intention wound healing or conventional sutures utilized in a particular technique. Serum albumin solders have been used *in vivo* and do not produce excessive inflammation.<sup>22,29,30</sup> We have utilized 2-octylcyanoacrylate in conjunction with the scaffold used here to recess extraocular rectus muscles in a rabbit model (unpublished results). Clinical observations over two weeks revealed no excessive ocular inflammation and histologic analysis at two weeks after surgery revealed no discernable inflammation in the area of application or reattachment.

The scaffold-enhanced light-activated solder described above can be easily utilized as a suture substitute in select ophthalmic surgical procedures. The use of a scaffold-enhanced light-activated solder also has advantages over other adhesives. First and foremost, the scaffold facilitates fine control over adhesive placement and tissue alignment. It provides an additional reinforcement for tensile strength and can act as a

slow-release drug delivery system following surgery. The ability to activate the solder with a specific wavelength of light permits long or large wounds to be closed very quickly and precisely. As well as the potential cost savings in suture products, operating room time may be reduced, especially in a resident teaching situation. Also, the time required to precisely align sutures under a microscope can be minimized. These savings are in addition to the ultimate goal of increasing the safety and efficacy of surgery for both the patient and the personnel performing the tasks.

In summary, we have demonstrated that the immediate tensile strengths achieved with scaffold-enhanced, light-activated solders are greater than those physiologically required for strabismus surgery and, very likely, for closure of scleral, corneal and conjunctival incisions as well. Further work is currently being performed by our group to assess the *in vivo* degradation rate of both the solder and the scaffold, in addition to their tensile strength, in strabismus surgery, corneal wound repair, scleral wound closure and conjunctival incisions. If the reduction of solder strength is sufficiently slow to allow inherent wound tensile strength to return to physiologic requirements, this technique may become widely used in many ophthalmic surgical applications.

**ACKNOWLEDGMENTS:**

This work was supported, in part, by an unrestricted grant from Research to Prevent Blindness, Inc. to the Department of Ophthalmology and Visual Sciences at the University of Illinois at Chicago, and, in part, by the Research Corporation through a Cottrell College Science Award, grant CC5010, by Lilly Endowment, Inc., through a Technology and Entrepreneurial Development Award, grant 960068, made to the Rose-Hulman Institute of Technology, and by an Eli Lilly Applied Life Sciences grant.

We wish to thank Marlos A.G.Viana, PhD, Department of Ophthalmology and Visual Sciences, University of Illinois at Chicago, for his assistance with the statistical analysis of this investigation.

## REFERENCES:

1. Noel LP, Bloom JN, Clarke WN, Bawazer A. Retinal perforation in strabismus surgery. *J Pediatr Ophthalmol Strabismus*. 1997;34:115-117.
2. Awad AH, Mullaney PB, Al-Hazmi A, Al-Turkmani S, Wheeler D, Al-Assaf M, et al. Recognized globe perforation during strabismus surgery: incidence, risk factors, and sequelae. *JAAPOS*. 2000;4:150-153.
3. Recchia FM, Bauman CR, Sivalingam A, Kleiner R, Duker JS, Vrabec TR. Endophthalmitis after pediatric strabismus surgery. *Ophthalmol*. 2000;118:939-944.
4. Rosenbaum AL. Endophthalmitis after strabismus surgery. *Arch Ophthalmol*. 2000;118:982-983.
5. Whitson WE, Weisenthal RW, Krachmer JH. Penetrating keratoplasty and keratoprosthesis; Tasman W, Jaeger EA (ed.); *Duane's Clinical Ophthalmology*, Philadelphia, Lippincott Williams and Wilkins; 2001, vol. 6, chap. 26, pp 1-28.
6. Vote BJ, Elder MJ. Cyanoacrylate glue for corneal perforations: a description of a surgical technique and a review of the literature. *Clin Experiment Ophthalmol*. 2000;28:437-442.
7. Taravella MJ, Chang CD. 2-Octyl cyanoacrylate medical adhesive in treatment of a corneal perforation. *Cornea*. 2001;20:220-221.

8. Spierer A, Barequet I, Rosner M, Solomon AS, Martinowitz U. Reattachment of extraocular muscles using fibrin glue in a rabbit model. *Invest Ophthalmol Vis Sci*. 1997;38:543-546.
9. Erbil H, Sinav S, Sullu Y, Kandemir B. An experimental study on the use of fibrin sealants in strabismus surgery. *Turk J. Pediatr*. 1991;33:111-116.
10. Ricci B, Ricci F, Bianchi PE. Octyl 2-cyanoacrylate in sutureless surgery of extraocular muscles: an experimental study on the rabbit model. *Graefe's Arch Clin Exp Ophthalmol*. 2000;238:454-458.
11. Gupta BK, Edward D, Duffy MT. 2-Octyl cyanoacrylate tissue adhesive and muscle attachment to porous anophthalmic orbital implants. *Ophthalm Plast Reconstr Surg*. 2001;17:264-269.
12. Burnstein AL, WuDunn D, Knotts SL, Catoira Y, Cantor LB. Conjunctival advancement versus nonincisional treatment for late-onset glaucoma filtering bleb leaks. *Ophthalmology*. 2002;109:71-75.
13. Wake MC, Gupta PK, Mikos AG. Fabrication of pliable biodegradable polymer foams to engineer soft tissues. *Cell Transplant*. 1996;5:465-473.
14. Menovsky T, Beek JF, van Gemert MJ. Laser tissue welding of dura mater and peripheral nerves: a scanning electron microscopy study. *Lasers Surg Med*. 1996;19:152-158.

15. Quinn J, Wells G, Sutcliffe T, Jarmuske M, Maw J, Stiell I, Johns P. A randomized trial comparing octylcyanoacrylate tissue adhesive and sutures in the management of lacerations. *JAMA*.1997;277:1527-1530.
16. Trott AT. Cyanoacrylate tissue adhesives. An advance in wound care. *JAMA*. 1997;277:1559-1560.
17. Detweiler MB, Detweiler JG, Fenton J. Sutureless and reduced suture anastomosis of hollow vessels with fibrin glue: a review. *J Invest Surg*. 1999;12:245-262.
18. Currie LJ, Sharpe JR, Martin R. The use of fibrin glue in skin grafts and tissue-engineered skin replacements: a review. *Plast Reconstr Surg*. 2001;108:1713-1726.
19. Shah MA, Ebert AM, Sanders WE. Fibrin glue fixation of a digital osteochondral fracture: case report and review of the literature. *J Hand Surg (Am)*. 2002;27:464-469.
20. Bass LS, Treat MR. Laser tissue welding: a comprehensive review of current and future clinical applications. *Lasers Surg Med*. 1995;17:315-349.
21. McNally-Heintzelman KM, Welch AJ. Laser tissue welding, in Vo-Dinh T (ed.) *Biomedical Photonics Handbook*; Boca Raton; CRC Press. (To be published Dec. 2002)

22. McNally KM, Sorg BS, Hammer DX, Heintzelman DL, Hodges DE, Welch AJ.  
Improved laser-assisted vascular tissue fusion using solder-doped polymer  
membranes on a canine model. *Proc SPIE*, 2000;3907:65-73.
23. McNally-Heintzelman KM, Riley JN, Dickson TJ, Hou DM, Rogers P, March KL.  
*In vivo* tissue repair using light-activated surgical adhesive on a porcine model.  
*Proc SPIE*, 2001;4244:226-232.
24. Holland SJ, Tighe BJ and Gould PL. Polymers for biodegradable medical devices.  
1. The potential of polyesters as controlled macromolecular release systems.  
*J Controlled Release*, 1986;4:155-180.
25. Reed AM, Gilding DK. Biodegradable polymers for use in surgery-  
poly(glycolic)/poly(lactic acid) homo and copolymers: 2. *In Vitro Degradation*.  
*Polymer*, 1981;22: 499-504.
26. McNally KM, Sorg BS, Welch AJ. Novel solid protein solder designs for laser-  
assisted tissue repair. *Lasers Surg Med*. 2000;27:147-157.
27. Collins CC, Carlson MR, Scott AB, Jampolsky A. Extraocular muscle forces in  
normal human subjects. *Invest Ophthalmol Vis Sci*. 1981;20:652-664.
28. Zieren J, Castenholz E, Baumgart E, Muller JM. Effects of fibrin glue and growth  
factors released from platelets on abdominal hernia repair with a resorbable PGA  
mesh: experimental study. *J Surg Res*. 1999;85:267-272.

29. Kirsch AJ, Cooper CS, Gatti J, Scherz HC, Canning DA, Zderic SA, et al.  
Laser tissue soldering for hypospadias repair: results of a controlled prospective clinical trial. *J Urol.* 2001;165:574-577.
30. Riley JN, Dickson TJ, Hou DM, Rogers P, March KL, McNally-Heintzelman KM.  
Improved laser assisted vascular tissue fusion using light-activated surgical adhesive in a porcine model. *Biomed Sci Instrum.* 2001;37:451-456.

Set	Adhesive Specifications
Set A (n=10)	25% BSA(w/v) ≤106 μm pore diameter
Set B (n=10)	25% BSA(w/v) 106 - 150 μm pore diameter
Set C (n=10)	50% BSA(w/v) ≤106 μm pore diameter
Set D (n=10)	50% BSA(w/v) 106 - 150 μm pore diameter

All sets used 0.5 mg/ml ICG, 85:15 PGLA, 70% wt. NaCl

**Table 1.** Adhesive fabrication parameters used in the study.

22/24

SPECIMEN #	GROUP A	GROUP B	GROUP C	GROUP D	NATIVE MUSCLE
1	256	365	310	371	419
2	237	381	390	582	629
3	262	435	301	480	504
4	275	390	256	464	557
5	240	326	272	432	497
6	253	397	262	422	498
7	256	410	266	477	563
8	230	336	346	358	437
9	227	352	301	378	438
10	275	365	307	368	401
MEAN (g)	251	376	301	433	494
STD DEV	17	34	42	70	73
% OF NATIVE TISSUE	51	76	61	88	100

**Table 2.** Maximum tensile strength (in grams) of scaffold-enhanced light-activated soldering of transected extraocular muscle-to-muscle according to adhesive and scaffold parameters outlined in Table 1.

SPECIMEN #	BREAKING LOAD (g)
1	284
2	279
3	302
4	295
5	254
6	296
7	343
8	367
9	294
10	290
11	286
12	230
13	257
14	288
15	229
16	287
17	280
18	338
19	326
20	366
Mean	295
St. Dev.	38

**Table 3.** Maximum tensile strength (in grams) of scaffold-enhanced light-activated soldering of sclera-to-sclera.

24/24

SPECIMEN #	BREAKING LOAD (g)
1	328
2	307
3	255
4	317
5	254
6	309
7	367
8	332
9	347
10	263
11	303
12	319
13	282
14	277
15	254
16	358
17	315
18	324
19	300
20	372
Mean	309
St. Dev.	37

**Table 4.** Maximum tensile strength (in grams) of scaffold-enhanced light-activated soldering of extraocular muscle-to-sclera.

## EXHIBIT B

### Conference: Tissue Sealants and Adhesives

#### LIGHT-ACTIVATED SURGICAL ADHESIVE: A SUTURELESS ALTERNATIVE FOR OPHTHALMIC SURGERY

Jeffrey N. Bloom, M.D.<sup>1</sup>, Mark T. Duffy, M.D., Ph.D.<sup>1</sup>, Jason B. Davis, B.S.<sup>2</sup>, and Karen M. McNally-Heintzelman Ph.D.<sup>2</sup>

<sup>1</sup>Department of Ophthalmology and Visual Sciences, University of Illinois at Chicago;

<sup>2</sup>Department of Applied Biology and Biomedical Engineering, Rose-Hulman Institute of Technology.

Ophthalmic surgery using sutures is technically demanding and time consuming, even in the hands of a skilled surgeon. Complications may arise from utilizing needles and suture during eye surgery. For example, intraoperative perforation of the sclera during strabismus surgery is a potentially vision threatening complication. Postoperative complications associated with other procedures such as corneal transplants, repair of corneal or scleral lacerations, and oculoplastic, glaucoma and retinal surgery may include wound leakage, foreign body or allergic reaction to sutures, corneal astigmatism, and suture tracts providing a portal of entry for microorganisms. A sutureless tissue repair alternative would eliminate many of these complications.

Three studies were performed to assess the feasibility of using a light-activated surgical adhesive composed of a poly(L-lactic-co-glycolic acid) scaffold doped with serum albumin and indocyanine dye in conjunction with an 808nm diode laser for improved tissue repair in several ophthalmic applications. These studies included bonding of the extraocular muscle to sclera (n=20), sclera to sclera (n=20) and transected muscle to muscle (n=10). The breaking load of the resulting bonds was assessed and determined to be  $308 \pm 36$  g,  $295 \pm 38$  g, and  $433 \pm 70$  g, respectively. While this study was limited to an *in vitro* investigation, these strengths were on the order of three to four times the maximum force to which these ocular tissues are normally subjected. Additionally, previous *in vivo* studies using this light-activated adhesive in vascular applications demonstrated a favorable histological profile with resorption of the adhesive material by seven days. The polymer membrane also offers the dynamic potential to be used as a delivery vehicle for antibiotics, growth factors or other pharmacologic agents to aid in the wound healing process and to decrease the risk of infection or neovascularization.

This light activated surgical adhesive has shown promising results in these initial feasibility studies. Extension of this study to include the cornea, would address the majority of surgeries in ophthalmology. Further investigation into the optimization of application parameters, as well as, adhesive composition for ophthalmic applications is the subject of ongoing studies.

#### For more information please contact:

Dr. Karen M. McNally-Heintzelman  
Biomedical Engineering Program  
Rose-Hulman Institute of Technology  
5500 Wabash Avenue, CM185  
Terre Haute, IN 47803  
Email: [karen.mcnally@rose-hulman.edu](mailto:karen.mcnally@rose-hulman.edu)

Dr. Jeffrey N. Bloom  
Department of Ophthalmology and Visual Sciences  
University of Illinois at Chicago  
1855 W. Taylor Street  
Chicago, IL 60612  
Email: [jbloom@uic.edu](mailto:jbloom@uic.edu)

# LIGHT-ACTIVATED SURGICAL ADHESIVE: A SUTURELESS ALTERNATIVE FOR OPHTHALMIC SURGERY

Jeffrey N. Bloom<sup>1</sup>, Mark T. Duffy<sup>1</sup>, Jason B. Davis<sup>2</sup> and Karen M. McNally-Heintzelman<sup>2</sup>

<sup>1</sup>Department of Ophthalmology and Visual Sciences, University of Illinois College of Medicine, Chicago, IL 60612  
<sup>2</sup>Biomedical Engineering Program, Rose-Hulman Institute of Technology, Terre Haute, IN 47803

## Motivation

Ophthalmic surgery is technically demanding and time consuming, even in the hands of a skilled surgeon and complications may arise from the use of needles and sutures during these procedures. For example, intraoperative perforation of the sclera during strabismus surgery is a potentially vision threatening complication. Postoperative complications associated with other procedures such as corneal transplants, repair of corneal or scleral lacerations, and ophthalmic glaucoma and retinal surgery may include wound leakage, foreign body or allergic reaction to sutures, corneal astigmatism, and sutures tracts providing a portal of entry for microorganisms. A sutureless tissue repair alternative would eliminate many of these complications.

These studies were performed to assess the feasibility of using a light-activated surgical adhesive composed of a poly(L-lactic-co-glycolic acid) scaffold doped with serum albumin and indocyanine dye in conjunction with an 808nm diode laser for improved tissue repair in several ophthalmic applications. These studies included bonding of transected extraocular muscle to extraocular muscle, sclera to sclera, and extraocular muscle to sclera.

## Materials and Methods

### Experimental Groups

Group	Attachment	Sample Size	Tissue Species
I	extraocular muscle to muscle	40	Rabbit
II	sclera to sclera	20	Human
III	extraocular muscle to sclera	20	Porcine

- Rabbit superior rectus extraocular muscles were harvested approximately 45 minutes after sacrificing the animals.
- Human sclera was obtained from the Indiana Lions Eye Bank, Inc.
- Porcine orbits were obtained from a slaughterhouse approximately 4 hours after sacrificing the animals.
- All tissue was stored in buffered phosphate solution at 4°C until required.

### Preparation of the Surgical Adhesive

- Bio-degradable polymer membranes of controlled porosity were fabricated using a solvent casting and particulate leaching technique.
- 200 mg of poly(L-lactic-co-glycolic acid) (PLGA) with a lactic glycolic acid ratio was dissolved in 2 ml of dichloromethane and mixed with NaCl in a 60 mm Petri dish.
- Protein solder was prepared with bovine serum albumin (BSA) and indocyanine (ICG) dye mixed with deionized water.
- Polymer membranes with dimensions of  $1.0 \times 0.80 \times 0.19$  mm were then left to soak for a minimum of two hours in the protein solder mix to form the surgical adhesive.
- Four sets of adhesive parameters were investigated:

Set	Adhesive Specifications
A	25% BSA (w/v); $\leq 106\mu\text{m}$ pore diameter
B	25% BSA (w/v); 106-150 $\mu\text{m}$ pore diameter
C	50% BSA (w/v); $\leq 106\mu\text{m}$ pore diameter
D	50% BSA (w/v); 106-150 $\mu\text{m}$ pore diameter

- All sets used 0.5 mg/ml ICG, 85:15 PLGA, 70% wt. NaCl

### Tissue Repair Procedure

#### GROUP I

- The approximate length and thickness of each muscle specimen was  $8.0 \times 1.5$  mm.
- A complete transection was accomplished with a scalpel and opposing ends were placed together.
- A strip of adhesive with dimensions of  $3.0 \times 1.0$  mm was used to join the tissue in conjunction with an 808-nm diode laser (Irad. = 15.5 W/cm<sup>2</sup>, spot-size = 1.0 mm, scan rate = 0.5 mm/s).

#### GROUP II

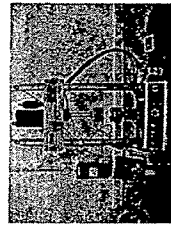
- Sclera tissue specimens with dimensions of  $4.0 \times 3.0$  mm were prepared.
- A full thickness incision was cut through the tissue specimen width using a scalpel and opposing ends were placed together.
- A strip of adhesive prepared using the optimal parameters determined in Group I (Set D) was used to repair the incisions in accordance with the procedure described above for Group I.

#### GROUP III

- A 360° conjunctival peritomy was performed on the globe exposing the points of muscle attachment and the superior rectus muscle was dissected from the globe using scissors.
- The rectus muscle was re-approximated to the sclera using a pair of forceps such that the end of the muscle was located adjacent to, but not overlying the original site of attachment.
- A piece of adhesive composed of the parameters outlined in Set D was applied across the top of the tissues in a head-to-tail fashion and the same repair procedure used for Group I was applied.

### Tensile Strength Analysis

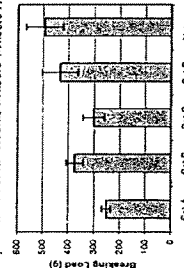
- The tensile strength of the resulting repairs was measured using a calibrated MTS Material Strength Testing Machine.
- The repaired tissue specimens were glued to small hooks attached to pneumatic grips which were in turn attached to a 500N load cell.
- Each specimen was pulled apart at a rate of 1 g/min until the repair failed.
- The maximum load in grams was recorded at the breaking point.



MTS Material Strength Testing Machine

## Results

### Group I: Extraocular Rectus Muscle-Muscle Adhesion



- Each bar represents mean and standard deviation of 10 repairs.
- Maximum strength achieved using Set D solder,  $433 \pm 70$  g.
- Strength of native tissue:  $494 \pm 73$  g.
- Statistical analysis demonstrated no interaction between pore size and albumin concentration.

### Group II: Sclera-Sclera Adhesion

- Average breaking load of sclera-sclera adhesions was  $295 \pm 38$  g.
- Mean modulus of elasticity of human scleral strips has previously been reported to be  $534 \pm 178$  g. (Fritberg *et al.*, Exp. Eye Res., 47:429-36, 1988.)

### Group III: Extraocular Rectus Muscle-to-Sclera Adhesion

- Average breaking load of sutureless muscle-sclera adhesions was  $309 \pm 37$  g.
- Mean active horizontal fixation force measured *in vivo* in humans at 50 degrees extreme gaze has previously been reported to be 74.8 g for the medial rectus muscle and 59.1 g for the lateral rectus muscle, with a range of 48 to 103 g for all individuals measured (Collins *et al.*, Invest. Ophthalmol. Vis. Sci. 20:652-64, 1981.)

## Discussion

- Immediate tensile strengths, although less than native tissue tensile strength, were comparable to those produced by suture repair.
- While this study was limited to an *ex vivo* investigation, these strengths were on the order of three to four times the maximum force to which these ocular tissues are normally subjected. Additionally, previous *in vivo* studies using this light-activated adhesive in vascular applications demonstrated a favorable histological profile with resorption of the adhesive material by seven days.

The scaffold-enhanced light-activated solder described above can be easily utilized as a suture substitute in most ophthalmic surgical techniques and offers many advantages over other adhesives as well.

- The scaffold facilitates fine control over tissue placement and alignment.
- The scaffold may act as an additional reinforcement in tensile strength and can provide a slow release drug delivery system for antibiotics, growth factors or other pharmacologic agents to aid in the wound healing process and to decrease the risk of infection or neo-vascularization.
- The ability to quickly and precisely activate the solder with a specific wavelength of light allows long or large wounds to be closed very quickly and precisely, reducing operating room time, and consequently, cost of the procedure.

## Future Directions

This light-activated surgical adhesive has shown promising results in these initial feasibility studies. Extension of this study to include the cornea, conjunctiva and eyelids would address a majority of ophthalmic surgeries. Further investigation into the optimization of application parameters, as well as, adhesive composition for ophthalmic applications is the subject of ongoing studies.

Additional work is also being performed to assess the *in vivo* rate of degradation of both the scaffold and the tensile strength in strabismus surgery, corneal wound repair and scleral wound closure. If the decrement of solder strength is sufficiently slow to allow inherent wound tensile strength to return to physiologic requirements, this technique may become widely used in many ophthalmic applications.

## Acknowledgments

This work was supported in part by an unrestricted grant from the Research to Prevent Blindness, Inc. to the Department of Ophthalmology & Visual Sciences at the University of Illinois at Chicago, and in part by Research Corporation through a Corneal College Sciences Award, grant CC3010, by Lilly Endowment, Inc., through a Technology and Entrepreneurial Development Award, grant 960068, made to Rose-Hulman Institute of Technology, and by an Eli Lilly Applied Life Sciences grant.

## EXHIBIT D

# Alternative Chromophores for Use in Light-Activated Surgical Adhesives

Brian D. Byrd <sup>a\*</sup>, Douglas L. Heintzelman <sup>b</sup> and Karen M. McNally-Heintzelman <sup>ah</sup>

<sup>a</sup> Biomedical Engineering Program, Rose-Hulman Institute of Technology, Terre Haute, IN 47803

<sup>b</sup> No affiliation

## ABSTRACT

A study was conducted to determine the feasibility of using alternative chromophores in light-activated surgical adhesives. Two commonly used chromophores, indocyanine green (ICG), and methylene blue (MB) were investigated, as well as three different food colorings: red #40, blue #1, and green food coloring consisting of yellow #5 and blue #1. The study consisted of three components. First, the absorption profiles of the five chromophores, both diluted in deionized water and bound to protein, were recorded with a UV-Vis-NIR spectrophotometer. Second, the effect of accumulated thermal dosages on the stability of the absorption profiles was investigated. Third, the stability of the absorption profiles of the chromophore solutions when exposed to ambient light for an extended period of time was investigated.

The peak absorption wavelengths of ICG, MB, red #40, and blue #1, were found to be 780 nm, 665 nm, 500 nm, and 630 nm respectively. The green food coloring had two absorption peaks at 417 nm and 630 nm, corresponding to the two dye components comprising this color. The peak absorption wavelength of the ICG shifted to 805 nm when bound to protein. ICG and MB showed a significant decrease in absorbance units with increased time and temperature when heated to temperatures up to 100 °C. Negligible change in absorption with accumulated thermal dose was observed for any of the three food colorings investigated. Photobleaching was observed in both ICG and MB solutions with exposure to a white light source. An 88% decrease in absorption was seen in ICG deionized water solution after 7 days of exposure with a corresponding 33% decrease in absorption seen in the MB deionized water solution. A negligible drop in absorption was observed from exposure to ambient light for a 12-week period with the three food colorings investigated.

**Keywords:** albumin protein solder, chromophore, laser soldering, tissue repair, absorption profile, accumulated thermal dose, degradation due to light exposure

## 1. INTRODUCTION

Many factors must be considered when selecting a chromophore to utilize in laser tissue soldering (LTS). The chromophore must have adequate absorption properties at an available laser wavelength. This means that the chromophore either needs to have a broad absorbance peak or have an absorption peak near the operating wavelength of the laser. Ideally the chromophore will provide for differential absorption between the dyed solder and the surrounding tissue, thus removing the requirement for precise focusing and aiming of the laser beam. The latter quality would also make it feasible to use much lower and safer laser irradiances. Examples of dyes that have been used to assist laser tissue repair procedures include carbon black and Fen 6 for use with Nd:YAG lasers,<sup>1-3</sup> indocyanine green for use with ~800nm diode lasers,<sup>4-8</sup> iron oxide and fluorescein for use with KTP frequency doubled Nd:YAG lasers,<sup>9,10</sup> and basic fuchsin, methyl violet, crystal violet, chlorin(c6) and fluorescein isothiocyanate for use with argon lasers.<sup>1,11-13</sup>

Knowledge of the optical penetration depth of the chromophore when mixed in protein solder is necessary to ensure adequate heat transmission through the full thickness of the solder. The decomposition products produced when the chromophore is irradiated with the laser energy, thus raising its temperature, must be safe. Finally, an understanding of how the chromophore degrades with time is necessary to ensure proper packaging of the product when taken to market. This degradation could include a decrease in the absorbance of the chromophore or a shift in the peak absorption wavelength. These factors determine the ultimate shelf life for the final product. Economic considerations relating to the cost of obtaining FDA

<sup>h</sup> For further information please contact Dr. Karen M. McNally-Heintzelman, Department of Applied Biology and Biomedical Engineering, Rose-Hulman Institute of Technology, 5500 Wabash Avenue, Terre Haute, IN 47803, Email: karen.mcnally@rose-hulman.edu

approval for use of the chromophore in the body, and the cost to procure, operate and maintain the corresponding laser system, are also important.

This work consists of three components. In the first component, the absorption profiles of the five chromophores were obtained when diluted in deionized water and when bound to protein and the peak absorption values and peak absorption wavelengths were evaluated. The second component investigated the effect of accumulated thermal dosages on the stability of the peak absorbance wavelengths and absorption peak values. The third component of the study explored the effect of prolonged exposure to ambient light on the absorption profiles of the five chromophores.

## 2. MATERIALS AND METHODS

### 2.1 Chromophore Absorption Profiles

#### 2.1.1 Preparation of Chromophore Solutions

Two commonly used chromophores, indocyanine green (ICG), and methylene blue (MB) were investigated, as well as three food colorings: red #40 (RFC), blue #1 (BFC), and green food coloring (GFC) consisting of yellow #5 and blue #1. Each of the five chromophores investigated were mixed with deionized water (Fisher Scientific, Hanover Park, IL) at five specified concentrations. The five chromophores and the concentrations used for each chromophore are summarized in Table 1.

Chromophore	Concentrations Investigated				
ICG	0.001 mg/mL	0.0025 mg/mL	0.005 mg/mL	0.0075 mg/mL	0.01 mg/mL
MB	0.001 mg/mL	0.0025 mg/mL	0.005 mg/mL	0.0075 mg/mL	0.01 mg/mL
RFC #40	0.5 $\mu$ L per 13 mL	1 $\mu$ L per 13 mL	5 $\mu$ L per 13 mL	10 $\mu$ L per 13 mL	20 $\mu$ L per 13 mL
BFC #1	0.5 $\mu$ L per 13 mL	1 $\mu$ L per 13 mL	5 $\mu$ L per 13 mL	10 $\mu$ L per 13 mL	20 $\mu$ L per 13 mL
GFC #5 & #1	0.5 $\mu$ L per 13 mL	1 $\mu$ L per 13 mL	5 $\mu$ L per 13 mL	10 $\mu$ L per 13 mL	20 $\mu$ L per 13 mL

Table 1: Chromophore concentrations tested in deionized water using cuvettes with a path length of 10mm.

These concentration ranges were determined experimentally by attempting to scan various concentrations of the chromophores with a UV-Vis-NIR spectrophotometer (Cary 500, Varian Inc., Walnut Creek, CA) until a concentration range was determined that was not too concentrated for the 10mm path length cuvettes (Sigma Chemical Company, St. Louis, MO) used in this portion of the study. This spectrophotometer is a double beam, ratio recording spectrophotometer that scans the sample and a blank simultaneously. Significantly higher chromophore concentrations suspended in deionized water created erroneous absorption profiles when used with the 10mm path length cuvettes. The preferred operating wavelength range for these cuvettes was 340 - 800 nm. Three stock solutions of each concentration were prepared for each of the five chromophores. Five samples of each chromophore concentration were then drawn from each of the three stock solutions and scanned with the spectrophotometer. Once the samples were prepared, they were transferred to the disposable polystyrene cuvettes with stoppers to prevent contamination from foreign matter. The filled cuvettes were stored in their original Styrofoam packaging to prevent light exposure and scratching of the cuvette surface. The samples were scanned with the spectrophotometer directly after preparation to minimize any degradation of the chromophore solution due to light exposure.

A smaller sample of much higher concentrations was investigated to determine if the peak absorption wavelength was concentration dependant. The five chromophores and the concentrations used for each chromophore are summarized in Table 2. A single stock solution was prepared for each chromophore and five samples of each concentration were scanned with the spectrophotometer. The cuvettes constructed for this study were prepared using microscope slides (Sigma Chemical Company) with a square cover slip sandwiched in between the slides at both ends of the slides. The slides were placed in a clamp and taped together at the ends after which the clamps were removed. The resultant path length of the cuvettes was  $0.15 \pm 0.02$  mm. The solution was pipetted into the void between the slides immediately before scanning to minimize any degradation of the chromophore solutions.

Chromophore	Concentrations Investigated				
ICG	0.1 mg/mL	0.25 mg/mL	0.5 mg/mL	0.75 mg/mL	1.0 mg/mL
MB	0.1 mg/mL	0.25 mg/mL	0.5 mg/mL	0.75 mg/mL	1.0 mg/mL
RFC #40	200 $\mu$ L per 13 mL	400 $\mu$ L per 13 mL	600 $\mu$ L per 13 mL	800 $\mu$ L per 13 mL	1000 $\mu$ L per 13 mL
BFC #1	200 $\mu$ L per 13 mL	400 $\mu$ L per 13 mL	600 $\mu$ L per 13 mL	800 $\mu$ L per 13 mL	1000 $\mu$ L per 13 mL
GFC #5 & #1	200 $\mu$ L per 13 mL	400 $\mu$ L per 13 mL	600 $\mu$ L per 13 mL	800 $\mu$ L per 13 mL	1000 $\mu$ L per 13 mL

Table 2: Chromophore concentrations tested in deionized water using cuvettes with a path length of 0.15 mm.

### 2.1.2 Preparation of Protein Solder

Examining the absorption profiles of the chromophores when bound to protein was the next aim of the study. Powdered bovine serum albumin was combined with the desired concentration of chromophore and deionized water to produce the protein solder. The chromophore concentrations used in this portion of the study were significantly higher than the concentrations used in the deionized water solutions. The range of ICG concentrations investigated was taken from studies in the literature using ICG-doped solid protein solders.<sup>6-10,14</sup> The concentration range for the other four chromophores was adjusted so that the absorbencies at the peak absorption wavelengths were roughly comparable to the ICG concentration range. The large increase in the chromophore concentration was caused by several factors. The 0.8mm path length of the solid solder was much shorter than the 10mm path length of the deionized water study. In addition, an increase in chromophore concentration was required to overcome the natural absorption peaks of the solder itself. The five chromophores and the concentrations used for each chromophore are summarized in Table 3. For each stock solution of chromophore and deionized water used to prepare the protein solder, five samples of each concentration were scanned with the spectrophotometer.

Chromophore	Concentrations Investigated				
ICG	0.1 mg/mL	0.25 mg/mL	0.5 mg/mL	0.75 mg/mL	1.0 mg/mL
MB	0.1 mg/mL	0.25 mg/mL	0.5 mg/mL	0.75 mg/mL	1.0 mg/mL
RFC #40	200 $\mu$ L per 13 mL	400 $\mu$ L per 13 mL	600 $\mu$ L per 13 mL	800 $\mu$ L per 13 mL	1000 $\mu$ L per 13 mL
BFC #1	200 $\mu$ L per 13 mL	400 $\mu$ L per 13 mL	600 $\mu$ L per 13 mL	800 $\mu$ L per 13 mL	1000 $\mu$ L per 13 mL
GFC #5 & #1	200 $\mu$ L per 13 mL	400 $\mu$ L per 13 mL	600 $\mu$ L per 13 mL	800 $\mu$ L per 13 mL	1000 $\mu$ L per 13 mL

Table 3: Chromophore concentrations tested in albumin solder with a path length of 0.8mm.

The solid protein solder was mixed using a 60% w/w percentage of albumin to deionized water until it obtained a putty like consistency. The resulting mixture was placed between two clear glass microscope slides and compressed using a parallel plate vice. The resulting protein sheets were  $0.8 \pm 0.02$  mm thick. The specimens were tested within a few hours of preparation to minimize any degradation due to light exposure.

### 2.2 Thermal Exposure of Chromophores

The next component of the study sought to determine if the chromophores are degraded by thermal exposure such as that experienced when irradiated with a laser. Hot water was chosen as the medium to deliver heat to the chromophore solutions. The water was heated in a cylindrical Pyrex pan with a diameter of 150 mm and a height of 75 mm. The Pyrex pan was placed on a laboratory hot plate with magnetic stirring rod capability. The stirring rod was utilized to minimize any temperature gradients in the water bath. The temperature of the water was measured by a laboratory thermometer suspended in the water bath away from the sides and bottom of the Pyrex pan. The water was heated to the desired temperature of 60, 80, or 100 °C. Once a steady state temperature was reached the temperature of the water bath was monitored constantly. Stock solutions were prepared in accordance with the methods described in Section 2.1.1. The stock solutions were then placed in 8mL glass vials with twist on lids. Two glass vials were suspended in the hot water bath for the allotted time period of 30, 60, 90, 120, 180, 240 or 300 s. The two vials contained enough solution to fill five cuvettes. The glass vials were removed from the hot water bath and immersed in an ice bath to quickly return the chromophore solutions to near room temperature. The sample solutions were then transferred to disposable polystyrene cuvettes with stoppers to keep out foreign matter. These filled cuvettes were stored in the lightproof Styrofoam container provided with the cuvettes until they were

scanned with the spectrophotometer. The samples were scanned immediately after the last sample had been prepared and immersed in the hot water bath. Five samples of each time, temperature, and chromophore combination were scanned with the spectrophotometer.

### 2.3 Light Exposure of Chromophores

The aim of this component of the study was to examine the effects of light exposure on the absorption profile of the selected chromophores. The experimental setup consisted of a lab bench with a desk lamp fitted with a standard 60W incandescent light bulb mounted on it. The desk lamp remained constantly illuminated throughout the light exposure study, and thus, it provided a constant source of illumination to model light exposure. A single stock solution of a single concentration for each chromophore was prepared as the experimental study group. The concentration used for the ICG and MB was 0.01mg/mL. The concentration used for the three food colorings was 20 $\mu$ L per 13mL. These concentrations were the highest concentrations tested in Section 2.1. These experimental stock solutions were placed in 130mL clear glass jars with the lids tightened firmly to prevent evaporation. The jars were placed in a single file line roughly a foot away from the bulb on the laboratory bench so that they were roughly perpendicular to the light source. Exposure periods were 0, 7, 14, 28, 56, and 84 days. A separate group of stock solutions were prepared using the same concentration as the experimental group to act as a control group. These control stock solutions were created to compare the degradation of the chromophore solutions without exposure to light. The control solutions were stored in amber glass bottles, which were then placed in a closed cardboard box to minimize light exposure to the chromophore solutions. A separate study containing only ICG and MB were tested daily from 0 to 7 days. Five samples of each chromophore were scanned with the spectrophotometer for each time period.

## 3. RESULTS

### 3.1 Chromophore Absorption Profiles

The absorption profiles of the five chromophores, both diluted in deionized water and bound to protein, were recorded with a Cary 500 UV-Vis-NIR spectrophotometer. Data were taken at 1 nm intervals over the spectrum range of 400 to 950nm.

#### 3.1.1 Chromophore Dissolved in Deionized Water

Typical absorption spectra for the highest concentration of each of the chromophores dissolved in deionized water and scanned with the long path length cuvettes (refer to Table 1) are shown below in Figure 1. The absorption spectra for the highest concentration used in the short path length study (refer to Table 2) are shown in Figure 2. The food colorings did not exhibit a characteristic shift in peak absorption wavelength with increased concentration in deionized water solution. The peak absorption of MB in deionized water solution decreased from 666 to 603 nm over the concentration range of 0.001 to 1.0 mg/mL. Likewise, the peak absorption of ICG in deionized water solution decreased from 781 to 698 nm over the concentration range of 0.001 to 1.0 mg/mL. This shift in peak absorption wavelength found in ICG and MB is caused by the progressive formation of aggregates as the concentration of the chromophore is increased.<sup>13,15,16</sup>

#### 3.1.2 Chromophore Bound to Serum Albumin

Typical absorption spectra for the highest concentration of each of the chromophores mixed with 60% w/w BSA protein solder (refer to Table 3) are shown below in Figure 3. At concentrations ranging from 0.001 to 0.01 mg/mL, the peak wavelength of the ICG spectrum displayed its characteristic shift from 780nm in deionized water to 805nm when bound to protein as discussed in previous studies.<sup>15</sup> A shift in peak absorption wavelength was also observed with MB. At a concentration of 1.0 mg/mL, the peak absorption of MB in deionized water was 603 nm, while when bound to protein, the peak absorption of MB was 665 nm (refer to Figures 2 and 3), similar to the lower concentration absorption spectra seen in Figure 1. No shift in the peak absorption wavelength of MB when bound to protein was seen for concentrations of 0.001 to 0.01 mg/mL. As seen in Figure 3, the shoulder of the MB spectra at approximately 615nm remains dominant in this higher concentration range when MB is bound to protein. The other three chromophores did not exhibit a shift in peak absorption wavelength when bound to protein.

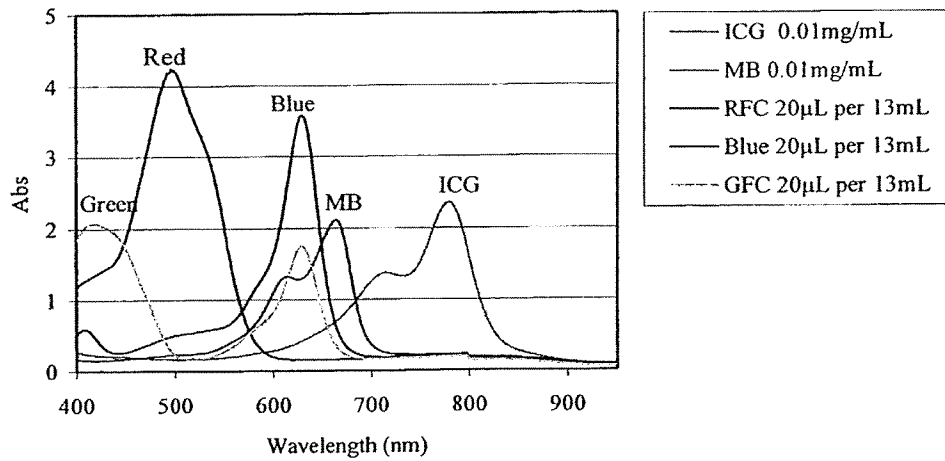


Figure 1: Typical absorption spectra of chromophores dissolved in deionized water (refer to Table 1) and scanned using cuvettes with a path length of 10 mm.

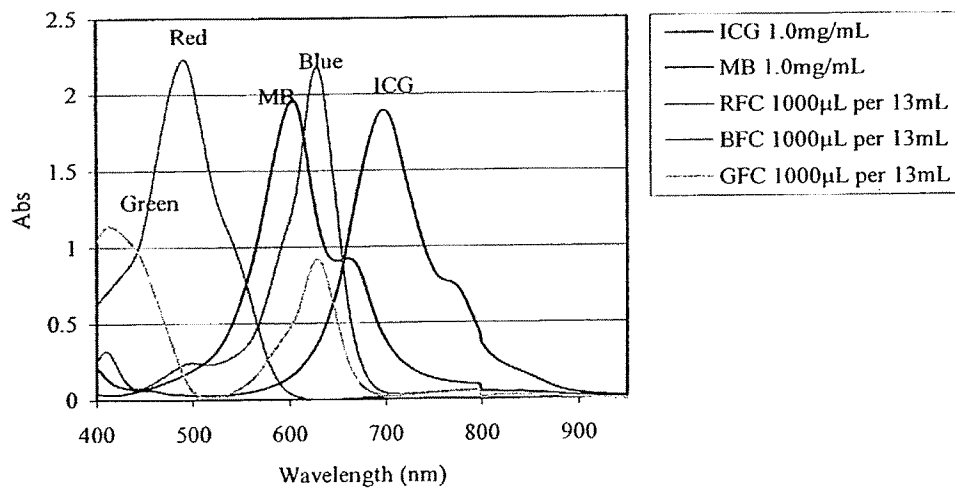


Figure 2: Typical absorption spectra of chromophores dissolved in deionized water (refer to Table 2) and scanned using cuvettes with a path length of 0.15 mm.

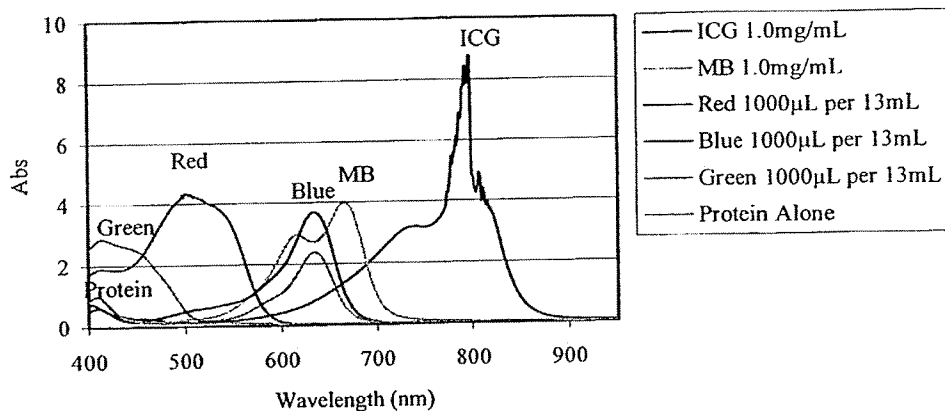


Figure 3: Typical absorption spectra for chromophores mixed with 60% w/w BSA protein solder (refer to Table 3). The path length of the solder specimens was 0.8 mm.

### 3.2 Effect of Thermal Denaturation in a Hot Water Bath

The results of the thermal denaturation study for each of the five chromophores investigated are presented in Tables 4 and 5. Table 4 presents the changes in absorbance at peak wavelength recorded when deionized water solutions containing ICG and MB were heated to temperatures of 60, 80, or 100 °C for various periods of time. Table 5 presents the changes in absorbance at peak wavelength recorded when deionized water solutions containing food coloring were heated to temperatures of 60 °C or 100 °C, for various periods of time. The ICG deionized water solutions experienced a 28% decrease in absorbance units after 300 seconds at 100 °C, the maximum thermal exposure investigated in this study. The remaining four chromophores experienced less than a 3.3% decrease in absorbance units after maximum thermal exposure. Although an analysis of variance test indicates a significant change in absorption with accumulated thermal dose for all temperature ranges of ICG, the 100 °C group showed a much larger decrease in absorbance units with increased time and temperature than the 60 °C and 80 °C groups. A negligible change in absorption with accumulated thermal dose was observed for MB and all of the food colorings investigated.

Time (sec)	ICG						MB					
	60 °C		80 °C		100 °C		60 °C		80 °C		100 °C	
	Mean	Std Dev	Mean	Std Dev	Mean	Std Dev	Mean	Std Dev	Mean	Std Dev	Mean	Std Dev
0	1.852	0.0400	1.852	0.0400	1.852	0.0400	2.237	0.0461	2.237	0.0461	2.237	0.0461
30	1.759	0.0941	1.707	0.0651	1.693	0.0487	2.120	0.0367	2.155	0.0215	2.238	0.0135
60	1.742	0.0813	1.652	0.0435	1.575	0.0956	2.144	0.0248	2.173	0.0353	2.234	0.0244
90	1.630	0.1504	1.670	0.0996	1.577	0.0561	2.049	0.0768	2.126	0.0991	2.204	0.0458
120	1.631	0.0786	1.742	0.0466	1.598	0.0631	2.095	0.0403	2.167	0.0920	2.184	0.0681
180	1.596	0.0376	1.712	0.0612	1.701	0.0576	2.180	0.0340	2.058	0.0948	2.134	0.0429
240	1.558	0.1002	1.735	0.0322	1.450	0.0771	2.147	0.0508	2.219	0.0156	2.170	0.0828
300	1.763	0.0355	1.714	0.0512	1.335	0.0851	2.145	0.0860	2.233	0.0366	2.188	0.0475

Table 4: Absorbance at peak wavelength recorded when deionized water solutions containing ICG and MB were heated to temperatures of 60, 80, or 100 °C for various periods of time.

Temperature of 60 °C

Time (sec)	RFC (500 nm)		BFC (630 nm)		GFC (417 nm)		GFC (630 nm)	
	Mean	Std Dev	Mean	Std Dev	Mean	Std Dev	Mean	Std Dev
0	4.341	0.01452	3.218	0.01452	2.082	0.06441	1.908	0.06309
60	4.262	0.04338	3.048	0.04338	2.070	0.07668	1.901	0.07236
180	4.185	0.03987	3.134	0.03987	2.070	0.03785	1.909	0.03550
300	4.255	0.01538	3.172	0.01538	2.109	0.00966	1.942	0.01131

Temperature of 100 °C

Time (sec)	RFC (500 nm)		BFC (630 nm)		GFC (417 nm)		GFC (630 nm)	
	Mean	Std Dev	Mean	Std Dev	Mean	Std Dev	Mean	Std Dev
0	4.341	0.03215	3.218	0.01452	2.082	0.06441	1.908	0.06309
60	4.320	0.02892	3.012	0.04338	2.014	0.08734	1.842	0.08739
180	4.132	0.08413	3.139	0.03987	2.051	0.04554	1.877	0.05066
300	4.252	0.07630	3.113	0.01538	2.080	0.02587	1.911	0.02584

Table 5: Absorbance at peak wavelength recorded when deionized water solutions containing blue, red and green food coloring were heated to temperatures of 60 °C or 100 °C for various periods of time.

**3.3 Degradation of Chromophore with Exposure to Light**

Several studies have explored the degradation of ICG solutions with exposure to light.<sup>16</sup> An initial study was conducted on the five chromophores being investigated in this study to evaluate possible degradation due to exposure to light. Experimental and control solutions (refer to Section 2.3) (two different stock solutions) were tested on days 0, 7, 14, 28, 56, and 84. The results of this study are presented in Table 6.

Experimental

	Day 0		1 week		2 weeks		4 weeks		8 weeks		12 weeks	
	Mean	Std Dev	Mean	Std Dev	Mean	Std Dev	Mean	Std Dev	Mean	Std Dev	Mean	Std Dev
ICG (780nm)	2.268	0.0615	0.3020	0.0201	0.2752	0.0239	0.2641	0.0198	0.2788	0.0080	0.1486	0.0471
MB (665 nm)	2.337	0.0166	1.722	0.0285	1.184	0.0110	0.3866	0.0216	0.2517	0.0105	0.1395	0.0619
RFC (500nm)	4.338	0.0338	4.413	0.0841	4.382	0.0741	4.413	0.0292	4.411	0.0579	4.209	0.0479
BFC (630nm)	3.650	0.0215	3.624	0.0201	3.579	0.0723	3.592	0.0473	3.649	0.0186	3.557	0.0354
GFC (417nm)	2.064	0.0527			2.068	0.0075			2.012	0.0268	1.978	0.0503
GFC (630nm)	1.758	0.0510			1.766	0.0060			1.698	0.0260	1.673	0.0492

Control

	Day 0		1 week		2 weeks		4 weeks		8 weeks		12 weeks	
	Mean	Std Dev	Mean	Std Dev	Mean	Std Dev	Mean	Std Dev	Mean	Std Dev	Mean	Std Dev
ICG (780nm)	2.033	0.0731	0.7964	0.0375	0.5252	0.0692	0.2937	0.0745	0.2104	0.0420	n/p	
MB (665 nm)	2.079	0.0386	2.117	0.0106	2.043	0.0674	1.994	0.0564	1.982	0.0246	2.043	0.0102
RFC (500nm)	5.756	0.2767	5.754	0.2098	5.754	0.2906	5.933	0.2655	5.644	0.2922	5.858	0.2648
BFC (630nm)	2.435	0.0685	2.499	0.0328	2.486	0.0718	2.460	0.0374	2.415	0.0293	2.436	0.0692
GFC (417nm)	2.221	0.0268	2.198	0.0503	2.242	0.0255	2.200	0.0389	2.148	0.0283	2.137	0.0724
GFC (630nm)	1.885	0.0278	1.857	0.0488	1.904	0.0278	1.864	0.0388	1.804	0.0227	1.792	0.0733

Table 6: Absorbance at peak wavelength recorded when deionized water solutions containing 0.01 mg/mL ICG and MB, and 20 µL per 13 mL RFC, BFC and GFC, were exposed to white light for a period up to 12 weeks.

The relatively quick degradation of the ICG and MB solutions compared to the food colorings prompted a shorter term study to evaluate the degradation of these two chromophores on a daily basis over a period of seven days of exposure. The results of this study are shown below in Figure 4. The ICG solution experienced the largest drop in absorbance during the first day in both the experimental and the control groups, with a total loss of absorbance of 87.5% over the seven-day period. MB experienced a 33% loss of its absorbance during the same period.

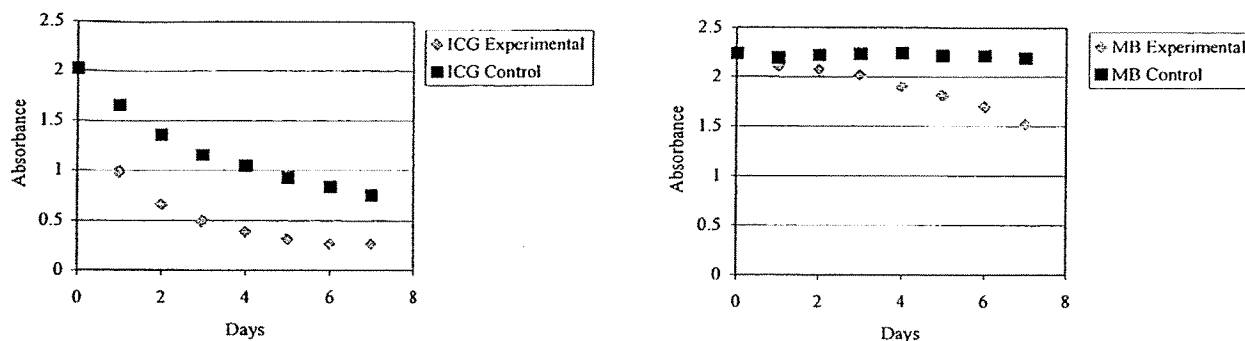


Figure 4: Absorbance at peak wavelength recorded when deionized water solutions containing 0.01 mg/mL ICG and MB were exposed to white light for a period up to 7 days.

#### 4. DISCUSSION

Three food colorings were explored for use as alternative chromophores in LTS. Selection criteria involved a close match between the absorption peak of the food coloring to be investigated with the operating wavelength of existing medical laser systems. Each of the food colorings had absorption peaks near the operating wavelength of existing medical lasers. The red food coloring had an absorption peak ( $\lambda = 500$  nm) that would allow it to be used with coumarin dye, Cu Vapor, Ar Ion, and Kr Ion lasers. The blue food coloring absorption peak ( $\lambda = 630$  nm) allows for its use with rhodamine dye, HeNe, Au Vapor, and Kr Ion lasers. The absorption peaks of the green food coloring ( $\lambda = 417$  nm and 630 nm) allow for its use with many different laser systems including a stilbene dye laser, or Kr Ion laser in addition to the lasers mentioned for use with the blue food coloring.<sup>19</sup> Each food coloring investigated demonstrated consistent peak absorption wavelengths when mixed either in deionized water solution or with albumin protein solder. Another attractive feature of these alternative chromophores is their lack of degradation due to heat and light exposure. Use of these chromophores would cause the protein in the solder to be the limiting factor on the shelf life of chromophore-doped protein solders.

Alteration of the concentration of ICG and MB from 0.001 to 0.01 mg/ml in deionized water produced a nearly linear increase in the chromophore absorbancies in accordance with the Beer-Lambert Law (BLL). The BLL is a core instrument in describing simple absorbance behavior of dilute solutions. This law is a simple linear relationship between absorbance,  $A$ , molar absorptivity,  $E$ , the path length of the light,  $L$ , and the concentration of the chromophore,  $C$ , where  $A \approx ELC$ . As the concentration of the solution becomes more concentrated aggregation of the dye molecules begins to occur. Several studies utilizing the optical properties of cyanine dyes indicate that the dye molecules dimerize as the concentration of the chromophore increases, resulting in the failure of Beer's Law.<sup>16</sup> In agreement with these studies, the linearity in absorbance was not observed when the concentrations of ICG and MB were increased beyond 0.01 to 1.0 mg/mL in deionized water. Likewise, the three food colorings did not follow the BLL over the broad range of concentrations investigated (0.5  $\mu$ L-1000  $\mu$ L per 13mL). The food colorings did, however, follow the BLL inside each of the separate concentration ranges investigated (0.5  $\mu$ L-20  $\mu$ L per 13mL and 200  $\mu$ L-1000  $\mu$ L per 13mL), independent of whether they were diluted in deionized water or in protein.

The peak absorption of ICG in deionized water solution decreased from 781 to 698 nm over the concentration range of 0.001 to 1.0 mg/mL. Likewise, the peak absorption of MB in deionized water solution decreased from 666 to 603 nm over the concentration range of 0.001 to 1.0 mg/mL. This shift in peak absorption wavelength has previously been noted by

Landsman *et al.*<sup>15</sup> The new peak wavelength can be seen as a shoulder around 695nm in the 0.01mg/mL spectra. The shoulder and the peak trade roles as the concentration of ICG is increased in the deionized water solution. MB behaves much in the same way as ICG. The shoulder occurring in the MB spectra around 615nm becomes the peak as the concentration of MB is increased in deionized water solution as discussed in Birch *et al.*<sup>13</sup> These shifts were first noted in the 0.1mg/mL deionized water solutions of ICG and MB, the lowest concentration used in the short path length study.

The peak absorption wavelength of 0.001 mg/mL ICG shifted from 781 nm in deionized water to 805 nm when mixed with 60%w/w albumin. The shift in peak absorption wavelength is due to the ICG binding to the protein in the solder. This protein binding interferes with the aggregation process.<sup>15,16</sup> The shift in wavelength needs to be considered when selecting an appropriate laser system to be used in conjunction with ICG. The most common laser system used with ICG is the AlGaAs semiconductor diode laser. While diode laser systems can be manufactured with peak wavelengths anywhere in the range of 750 – 1550 nm, many hospitals are equipped with a 780nm diode laser having a full-width half-max range of only 15 nm. Such a system would be suitable for use with ICG in deionized water solution, however, they would not be very suitable for use with ICG-doped protein solders.

ICG showed a significant decrease in absorbance units with increased time and temperature when heated up to temperatures of 100 °C. This observation was consistent with data presented by Dimitrov *et al.*<sup>17</sup> In Dimitrov's study, ICG mixed with 2.5% human serum albumin (HSA) was exposed to a hot water bath of 80 °C and 100 °C for a period up to 4 hours. The absorbance of specimens heated at 80 °C dropped from 2.56 to 2.53, 2.44, and 2.35 after 1, 2 and 4 hours, respectively. Specimens heated at 100 °C dropped from 2.63 to 2.58, 2.45 and 1.83 after 1, 2 and 4 hours, respectively. While the overall decrease in absorbance was not as significant in the present study, most likely due to the much shorter thermal exposure times investigated, the decrease in absorption per unit time was greater than that found in Dimitrov's study. This observation may be due to the fact that HSA has been found to impede the degradation of ICG<sup>16,18</sup>. The absorbance of ICG specimens heated at 100 °C in the present study dropped from 1.85 to 1.34 after a period of 300 s. The time frame investigated in the present study is more consistent with that used in LTS applications. Although statistically all of the chromophores were in some way affected by temperature, the difference in absorption of ICG and MB was much more evident in this time frame than it was for the three food colorings investigated. Use of the alternative chromophores seems advantageous due to the improved stability of their absorption profiles with accumulated thermal dosages.

Studies performed by Zhou *et al.* indicate that ICG solutions exposed to light degrade more quickly than those kept in the dark.<sup>16</sup> In the present study, the absorbance of ICG in deionized water solution fell from 2.02 to 1.06 after only one day of exposure to white light, and to 0.26 after seven days of exposure. In comparison, the absorbance of the control solution fell to 1.69 and 0.75 after one and seven days, respectively. A study performed by Gathje *et al.* indicates that HSA impedes the degradation of ICG when exposed to light.<sup>18</sup> The concentration's of ICG and serum albumin that are typically used in LTS applications are much higher than those used in the Gathje study. The stability of ICG was said to increase in albumin concentrations up to 3% with stability decreasing if albumin concentrations were increased past that level.<sup>18</sup> Likewise, MB also experiences some degradation from exposure to light. The absorbance of the MB solution fell from 2.24 to 2.15 after one day of exposure to white light, and to 1.48 after seven days of exposure. In comparison, the absorbance of the control solution fell to 2.13 and 2.17 after one and seven days, respectively. The absorption profiles of ICG and MB experimental groups as well as the ICG control group had no discernable peaks after 84 days. The MB control group maintained its absorbance after 84 days (refer to Table 6). The red, blue, and green food coloring did not display a large loss of absorption after 84 days. This property makes the food colorings particularly attractive for LTS applications as, in contrast to ICG and MB, the chromophores would not be the limiting factor on determining the shelf life of the protein solders.

## 5. CONCLUSION

The purpose of this study was to investigate the absorption properties for three common, easily obtained chromophores for use in LTS applications. The absorption properties were evaluated under various conditions including diluted in deionized water, when bound to protein, after accumulated thermal dosages and after extended light exposure. The properties of these alternative chromophores appear to have attractive qualities compared to the commonly used ICG. The alternative chromophores do not degrade in a deionized water solution with exposure to ambient light, nor do they degrade with time. These results are encouraging for improving LTS. Future studies will include exploration of the decomposition products of these chromophores when used in tissue and irradiated with laser energy. A tensile strength analysis will also be conducted to compare the strength of repairs formed using these new chromophore-enhanced protein solders with the strength of repairs formed using ICG and MB enhanced protein solders.

## ACKNOWLEDGMENTS

The authors thank Dr. Daniel Morris, Rose-Hulman Institute of Technology, for his assistance and guidance with the spectrophotometer; and Mr. Gary Burgess, Rose-Hulman Institute of Technology, for his assistance in fabricating the laboratory fixtures used to produce the solid protein solder sheets

This work was supported in part by Research Corporation through a Cottrell College Science Award, grant CC5010, by Lilly Endowment, Inc. through the Technology and Entrepreneurial Development, grant 960068, made to Rose-Hulman Institute of Technology, and by an Eli Lilly Applied Life Sciences grant.

## REFERENCES

1. Brooks SG, Ashley S, Fisher J, Davies GA, Griffiths J, Kester RC and Rees MR, "Exogenous Chromophores for the Argon and Nd:YAG Lasers: A Potential Application to Laser-Tissue Interactions", *Lasers. Surg. Med.*, **12(3)**:294-302, 1992.
2. Kokosa JM, Przjazny A, Bartels KE, Motamedi ME, Hayes DJ, Wallace DB and Frederickson CJ, "Laser-Initiated Decomposition Products of Indocyanine Green (ICG) and Carbon Black Sensitized Biological Tissues," *Proc. SPIE*, **2974**:205-213, 1997.
3. Fried NM and Walsh JT, Jr, "Laser Skin Welding: In Vivo Tensile Strength and Wound Healing Results," *Lasers. Surg. Med.*, **27(1)**:55-65, 2000.
4. Oz MC, Bass LS, Popp HW, Chuck RS, Johnson JP, Trokel SL and Treat MR, "In Vitro Comparison of Thulium-Holmium-Chromium:YAG and Argon Ion Lasers for Welding Biliary Tissue," *Lasers. Surg. Med.*, **9(3)**:248-253, 1989.
5. Poppas DP, Wright EJ, Guthrie PD, Shlahet LT and Retik AB, "Human Albumin Solders for Clinical Application During Laser Tissue Welding," *Lasers. Surg. Med.*, **19(1)**:2-8, 1996.
6. McNally KM, Sorg BS, Chan EK, Welch AJ, Dawes JM and Owen ER, "Optimal Parameters for Laser Tissue Soldering. Part I: Tensile Strength and Scanning Electron Microscopy Analysis," *Lasers. Surg. Med.*, **24(5)**:319-331, 1999.
7. Xie H, Shaffer BS, Prah SA and Gregory KW, "Laser Welding With an Albumin Stent: Experimental Ureteral End-to-End Anastomosis", *Proc. SPIE*, **3907**:215-220, 2000.
8. Kirsch AJ, Cooper CS, Gatti J, Scherz HC, Canning DA, Zderic SA and Snyder HM, "Laser Tissue Soldering for Hypospadias Repair: Results of a Controlled Prospective Clinical Trial", *J. Urol.*, **165(2)**:574-577, 2001.
9. Poppas D, Sutaria P, Sosa RE, Mininberg D and Scholssberg S, "Chromophore Enhanced Laser Welding of Canine Ureters in Vitro Using a Human Protein Solder: A Preliminary Step for Laparoscopic Tissue Welding", *J. Urol.*, **150**:1052-1055, 1993.
10. Wright EJ and Poppas DP, "Effect of Laser Wavelength and Protein Solder Concentration on Acute Tissue Repair Using Laser Welding: Initial Results in a Canine Ureter Model", *Tech. Urol.*, **3(3)**:176-181, 1997.
11. Self AB, Coe DA and Seeger JM, "Limited Thrombogenicity of Low Temperature, Laser-Welded Vascular Anastomoses", *Lasers. Surg. Med.*, **18(3)**:241-247, 1996.
12. Khadem J, Veloso AA Jr, Tolentino F, Hasan T and Hamblin MR, "Photodynamic Tissue Adhesion With Chlorin(e6) Protein Conjugates", *Invest. Ophthalmol. Vis. Sci.*, **40(13)**:3132-3137, 1999.
13. Birch JF, Mandley DJ, Williams SL, Worrall DR, Trotter PJ, Wilkinson F and Bell PR, "Methylene Blue Based Protein Solder for Vascular Anastomoses: An in Vitro Burst Pressure Study", *Lasers Surg. Med.*, **26(3)**:323-329, 2000.
14. Riley JN, McNally-Heintzelman KM, Hammer DX, Heintzelman DL, Sorg BS, Hodges DE and Welch AJ, "Application of a New Range of Light-Activated Surgical Adhesives for Vascular Repair in a Canine Model," *Int. J. Cardio. Med. Sci.*, **3(3-4)**:135-138, 2000.
15. Landsman MLJ, Kwant G, Mook GA and Zijlstra WG, "Light-Absorbing Properties, Stability, and Spectral Stabilization of Indocyanine Green," *J. Appl. Physiol.*, **40(4)**:575-583, 1976.

16. Zhou JF, Chin MP and Schafer SA, "Aggregation and Degradation of Indocyanine Green," *Proc. SPIE*, 2128:495-505, 1994.
17. Dimitrov D, Bass LS and Treat MR, "Thermal Breakdown Properties of Indocyanine Green" *Proc. SPIE*, 2395:486-489, 1995.
18. Gathje J, Steuer R and Nicholes KRK, "Stability Studies on Indocyanine Green Dye." *J. Appl. Physiol.* 29: 181-185, 1970
19. Katzir A, *Lasers and Optical Fibers in Medicine*. New York. Academic Press Inc. 1993.

## EXHIBIT E

## Alternative Chromophores for use in Light-Activated Surgical Adhesives: Optimization of Parameters for Tensile Strength and Thermal Damage Profile

Grant T. Hoffman <sup>a\*</sup>, Brian D. Byrd <sup>a</sup>, Eric C. Soller <sup>a</sup>, Douglas L. Heintzelman <sup>b</sup>  
and Karen M. McNally-Heintzelman <sup>a#</sup>

<sup>a</sup> Biomedical Engineering Program, Rose-Hulman Institute of Technology, Terre Haute, IN 47803

<sup>b</sup> No affiliation

### ABSTRACT

The use of indocyanine green-doped albumin protein solders has been shown to vastly improve the anastomotic strength that can be achieved by laser tissue repair techniques, while at the same time minimizing collateral thermal tissue damage. However, the safety of the degradation products of the chromophore following laser irradiation is uncertain. Therefore, we studied the feasibility of using alternative chromophores in terms of temperature rise at the solder/tissue interface, the extent of thermal damage in the surrounding tissue, and the tensile strength of repairs. Biodegradable polymer scaffolds of controlled porosity were fabricated with poly(L-lactic-co-glycolic acid), using a solvent-casting and particulate-leaching technique. The porous scaffold acted as a carrier to the traditional protein solder composition of serum albumin and an absorbing chromophore mixed in deionized water. Two commonly used chromophores, indocyanine green and methylene blue were investigated, as well as blue and green food colorings.

Temperature rise at the solder surface and at the interface between the solder and tissue were monitored by an IR temperature monitoring system and a type-K thermocouple, respectively, and the extent of thermal damage in the underlying tissue was determined using light microscopy. As expected, temperature rise at the solder/tissue interface, and consequently the degree of collateral thermal tissue damage, was directly related to the penetration depth of the laser light in the protein solder. Optimal tensile strength of repairs was achieved by selecting a chromophore concentration that resulted in a temperature of  $66 \pm 3$  °C at the solder/tissue interface.

**Keywords:** laser tissue repair, albumin solder, alternative chromophores, indocyanine green, methylene blue, food coloring, polymer scaffold, poly(L-lactic-co-glycolic acid), infrared temperature monitoring system, tensile strength

### 1. INTRODUCTION

The feasibility of laser tissue welding was first demonstrated in 1979 when Jain *et al.* successfully joined small blood vessels together using a neodymium laser.<sup>1</sup> Since then, researchers have been searching for ways to establish this method of sutureless tissue repair into common medical practice. The advantages of laser-assisted tissue repair include reduced inflammation and foreign body response, liquid-tight seals, faster healing, and the potential for simpler methods of minimally invasive and endoscopic tissue closure. Despite a substantial amount of research in the field, clinical acceptance of laser welding techniques has been hindered by such obstacles as poor strength and reproducibility of the repairs, thermal damage to the tissue, and ambiguous and arbitrary end-points in the welding process. The addition of protein solders composed of various exogenous materials including blood,<sup>2</sup> albumin,<sup>3</sup> and collagen<sup>4</sup> and elastin<sup>5</sup>-based patches, has improved weld strength and the reproducibility of the technique. The addition of wavelength-specific chromophores including indocyanine green (ICG),<sup>6-11</sup> methylene blue (MB),<sup>12</sup> and carbon black (CB)<sup>13</sup> has provided for differential absorption between the dyed region and the surrounding tissue, thus minimizing thermal damage to the underlying tissue caused by unwanted absorption of the laser energy. Finally, the use of a biodegradable polymer scaffolding as a carrier for the solder is an emerging technique shown to improve the success rate and repeatability of the laser welding technique.<sup>11</sup>

<sup>#</sup> For further information please contact Dr. Karen M. McNally-Heintzelman, Department of Applied Biology and Biomedical Engineering, Rose-Hulman Institute of Technology, 5500 Wabash Avenue, Terre Haute, IN 47803, Email: karen.mcnally@rose-hulman.edu

Questions regarding the safety of the decomposition products of ICG when heated to temperatures above 60 °C has caused some concern amongst researchers and clinicians alike.<sup>14</sup> Further analysis is required to determine if these decomposition products are substantially different to those that we are exposed to on a day-to-day basis when, for example, we consume food that is slightly carbonized (burnt). In the meantime, the questionable nature of these commonly used chromophores has prompted a search for alternative chromophores to be used in laser tissue welding procedures mediated by a protein solder. The purpose of this study was thus to determine the feasibility of using alternative chromophores in terms of temperature rise at the solder/tissue interface, the extent of thermal damage in the surrounding tissue, and the tensile strength of repairs. Two commonly used chromophores, ICG and MB were investigated, as well as two different food colorings: blue #1, and green food coloring consisting of yellow #5 and blue #1.

## 2. MATERIALS AND METHODS

### 2.1 Preparation of Chromophore-Enhanced Solder-Doped Scaffolds

Protein solder was prepared by combining 50% bovine serum albumin (BSA) (Sigma Chemical Company, St. Louis, MO) with the desired concentration of chromophore in deionized water. The four chromophores, ICG, MB, blue food coloring (BFC) and green food coloring (GFC), and the concentrations used for each chromophore, are summarized in Table 1 below. The range of ICG concentrations investigated was taken from studies in the literature using ICG-doped protein solders.<sup>7-11</sup> The concentration range for the other four chromophores was adjusted such that the absorption at the peak absorption wavelengths were roughly comparable to those observed within the range of ICG concentrations. The solder was placed in light-proof plastic vials and stored at 4 °C until needed. Solder remaining after three days was discarded.

Chromophore	Concentrations Investigated				
ICG	0.1 mg/mL	0.25 mg/mL	0.5 mg/mL	0.75 mg/mL	1.0 mg/mL
MB	0.1 mg/mL	0.25 mg/mL	0.5 mg/mL	0.75 mg/mL	1.0 mg/mL
BFC (#1)	200 $\mu$ L per 13 mL	400 $\mu$ L per 13 mL	600 $\mu$ L per 13 mL	800 $\mu$ L per 13 mL	1000 $\mu$ L per 13 mL
GFC (#5 + #1)	200 $\mu$ L per 13 mL	400 $\mu$ L per 13 mL	600 $\mu$ L per 13 mL	800 $\mu$ L per 13 mL	1000 $\mu$ L per 13 mL

Table 1: Chromophore concentrations tested in chromophore-enhanced solder-doped scaffolds.

Porous synthetic polymer scaffolds were fabricated using poly(L-lactic-co-glycolic acid) (PLGA) with a solvent casting and particulate leaching technique.<sup>15</sup> Two hundred milligrams PLGA (Sigma Chemical Company) was dissolved in dichloromethane and subsequently mixed with 467 milligrams sodium chloride (70% weight fraction, particle size 106-150  $\mu$ m). The polymer was then poured into a 60mm diameter Petri dish and left beneath a fume hood for 24 hours to allow the dichloromethane to evaporate. Upon drying, the scaffolds were immersed in deionized water three to four times over a 24-hour period to leach out the salt particles, leaving behind the porous polymer scaffolds. After removing the scaffolds from the Petri dishes, they were left to air dry and then stored until needed. Prior to use for tissue repairs, the polymer scaffolds were cut into 10 mm by 5 mm rectangular pieces and subsequently soaked in the BSA protein solder for two hours. The thicknesses of the chromophore-enhanced solder-doped scaffolds, determined by scanning electron microscopy and measurement with precision calipers (L.S. Starrett Co., Anthol, MA), were in the range of 145 to 155  $\mu$ m.

### 2.2 Optical Penetration Depth of Laser Light in Chromophore-Enhanced Solder-Doped Scaffolds

The peak absorption wavelengths of ICG, MB and BFC when bound to protein have previously been determined to be 805 nm, 665 nm, and 630 nm, respectively.<sup>16</sup> The GFC had two absorption peaks at 417 nm and 630 nm, corresponding to the two dye components comprising this color. The lasers available for use in this study were a 5W 808nm diode laser (Spectra Physics, Mountain View, CA) for use with ICG, a 400mW 670nm diode laser (Coherent Inc., Santa Clara, CA) for use with MB, and a 35mW 632.8nm diode laser (Coherent Inc.) for use with BFC and GFC.

Specimens of the chromophore-enhanced solder-doped scaffolds were pressed between two glass slides to form a slab having dimensions  $\geq 2 \times 2$  cm with an approximate thickness of 150  $\mu$ m. Total transmission and diffuse reflection were measured on five samples of each of the chromophore-enhanced solder-doped scaffold specimens using a UV-Vis-NIR spectrophotometer (Cary 500, Varian Instruments, Walnut Creek, CA), equipped with an integrating sphere. The diffusion approximation with a

delta-Eddington phase function<sup>17</sup> that assigns forward scattered light into a delta function, and the predetermined refractive indices for albumin protein solder reported in a previous study<sup>18</sup>, were input into Prah's iterative program for inverse adding-doubling<sup>19</sup> to determine the absorption and reduced scattering coefficients of each of the chromophore-enhanced solder-doped scaffolds. The program computed the diffuse reflection and total transmission for an assumed pair of values for absorption and reduced scattering coefficients. Prah's program considered multiple reflections that occurred at air/slide/solder/slide/air interfaces. New values of the absorption coefficient,  $\mu_a$  (in inverted meters), and the reduced scattering coefficient,  $\mu_s' = \mu_s(1-g)$  (in inverted meters), were automatically computed until reflection and transmission matched measured values. The scattering coefficient,  $\mu_s$ , was also calculated with the anisotropy factor,  $g$  (no units), assumed to be  $\sim 0.80$ , as determined for BSA solder in a previous study.<sup>20</sup> From these measurements, the optical penetration depth (OPD) ( $\delta = 1/(\mu_a + \mu_s')$ ) in the chromophore-enhanced solder-doped scaffolds of each of the corresponding laser wavelengths was calculated for a thickness of approximately 150  $\mu\text{m}$ .

### 2.3 Laser-Solder Repair Technique

Bovine thoracic aortas were obtained from a local slaughterhouse. The aortas were washed in phosphate buffered saline and cut into rectangular pieces with dimensions of  $2.5 \times 1.5$  cm. The excess adventitia was trimmed to obtain a specimen thickness of approximately 1 mm. Laser-soldering was conducted on the intima of the aorta. A full thickness incision was cut through the specimen width using a scalpel and opposing ends were placed together. A strip of chromophore-enhanced solder-doped scaffold was then placed over the incision and thermally bonded to the tissue by means of light activation with the corresponding laser. Each laser was operated in continuous mode with a spot-size at the solder surface of approximately 1 mm for the 808nm and 670nm diode lasers, and 0.5 mm for the 632.8nm diode laser. An irradiance of approximately  $15.9 \text{ W/cm}^2$ , measured using a Fieldmaster GS power meter with a LM100 thermopile detector (Coherent Scientific, Santa Clara, CA), was delivered to the surface of the solder. The laser beam was scanned in a continuous spiral pattern across the solder two times (starting from the center). The approximate exposure time for each repair was  $80 \pm 5$  s. Ten repairs were performed for each set of parameters investigated (refer to Table 1).

### 2.4 Temperature Analysis

#### 2.4.1 Solder Surface and Solder/Tissue Interface Temperature Measurements

The temperature of the solder surface was monitored during the laser procedure using an IR temperature monitoring system designed by the authors. The system measured blackbody radiation emitted from the weld site with an infrared pyroelectric detector. The blackbody radiation was guided from the weld site to the radiometer via a silver halide ( $\text{AgCl}_x\text{AgBr}_{1-x}$ ) core-clad fiber (courtesy of Abraham Katzir, Tel Aviv University, Israel) which had a core diameter of 700  $\mu\text{m}$ . The laser delivery and radiometer fibers were held together using a custom hand-piece that allowed the fibers to be fixed facing the same spot. The system had a response time of 10 ms and the minimum resolvable temperature difference was 1  $^\circ\text{C}$ . The system was calibrated over the range of 30 to 150  $^\circ\text{C}$  using black bodies of known temperature and using the assumption that the emissivity of the solder was approximately equal to 1.0. The temperature at the solder/tissue interface was monitored during the laser procedure using a 0.5mm type-K thermocouple. The thermocouple had a response time of 50 ms and the minimum resolvable temperature difference was 0.5  $^\circ\text{C}$ .

#### 2.4.2 Light Microscopy

Light microscopy was used to determine the depth of thermal damage in the underlying tissue substrate as a result of the laser treatment. Masson's Trichrome and Hematoxylin and Eosin (H&E) were used as the staining agents. The depth of damage in the tissue substrates was estimated using two criteria: (i) a color change in the tissue collagen from green to crimson (Masson's Trichrome staining) signifying denaturation, and (ii) structural variations such as swelling of collagen fibers in the tissue (Hematoxylin and Eosin staining). The more subtle indications of damage including cellular shrinkage and conformational changes were neglected. Uncertainty in the measurements is attributed to variations in the level of staining achieved with the different batches of stains and small variations in the physiological structure of individual specimens.

## 2.5 Tensile Strength Analysis

Tensile strength measurements were performed to test the integrity of the resultant repairs immediately following the laser procedure using a calibrated MTS Material Strength Testing Machine (858 Table Top System, MTS, Eden Prairie, MN). This system was interfaced with a personal computer to collect the data. Each tissue specimen was clamped to the strength testing machine using a 500N load cell with pneumatic grips. The specimens were pulled apart at a rate of 1gf/sec until the repair failed. Complete separation of the two pieces of tissue defined failure. The maximum load in grams was recorded at the breaking point. In order to avoid variations in repair strength associated with drying, the tissue specimens were kept moist during the procedure.

## 3. RESULTS

The OPD's of each of the four chromophores are presented in Figures 1a and 1b as a function of chromophore concentration. As specified in Section 2.1, the thicknesses of the solder-doped polymer scaffolds were in the range of 145 to 155  $\mu\text{m}$ .

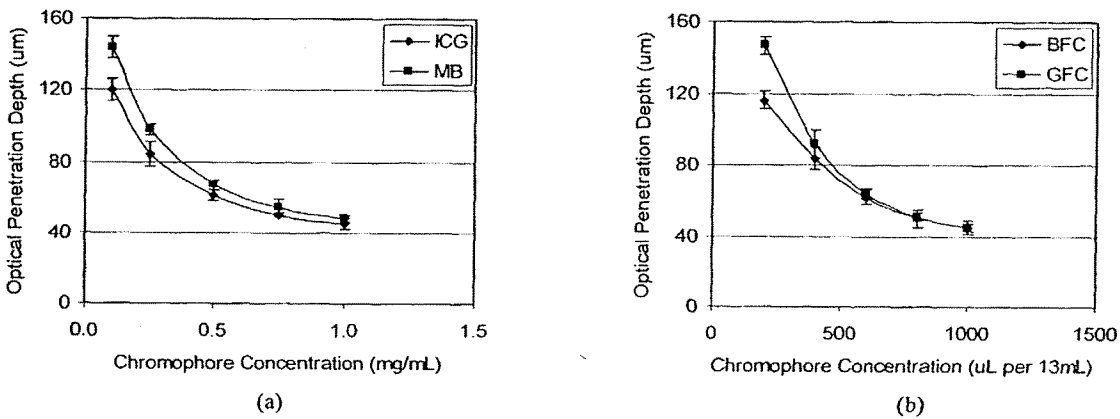


Figure 1: (a) OPD of 808nm light in ICG-enhanced and 670nm light in MB-enhanced solder-doped polymer scaffolds. (b) OPD of 632.8nm light in BFC-enhanced and GFC (#1)-enhanced solder-doped polymer scaffolds. The thickness of the solder-doped polymer scaffolds was approximately 150  $\mu\text{m}$ . Each point represents the mean and standard deviation for five specimens.

Figure 2 presents the results of studies conducted to determine the temperature at the solder/tissue interface and the degree of collateral thermal damage in the underlying tissue as a result of the laser procedure. As can be seen in these graphs, temperature rise at the solder/tissue interface, and consequently the degree of collateral thermal tissue damage, was directly related to the penetration depth of laser light in the chromophore-enhanced solder-doped scaffold.

The tensile strength of repairs performed using the chromophore-enhanced solder-doped scaffolds are presented in Figure 3 as a function of the temperature reached at the solder/tissue interface during the laser procedure. The tensile strength of repairs was optimized by selecting a chromophore concentration that resulted in a temperature of  $66 \pm 3^\circ\text{C}$  at the solder/tissue interface. The optimal concentrations were 0.5mg/mL for ICG and MB, and 600 $\mu\text{L}$  per 13mL for BFC (#1) and GFC (#1). At these concentrations, the OPD's were recorded to be  $61 \pm 3 \mu\text{m}$ ,  $67 \pm 3 \mu\text{m}$ ,  $62 \pm 4 \mu\text{m}$  and  $64 \pm 3 \mu\text{m}$ , respectively.

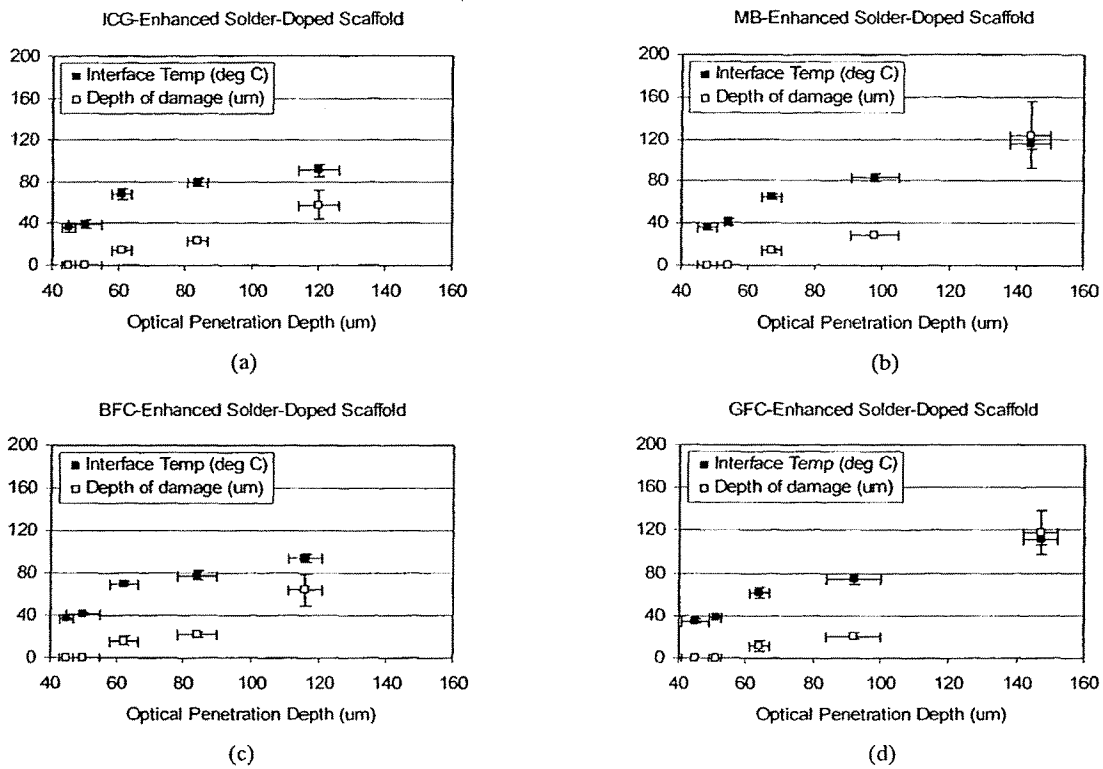
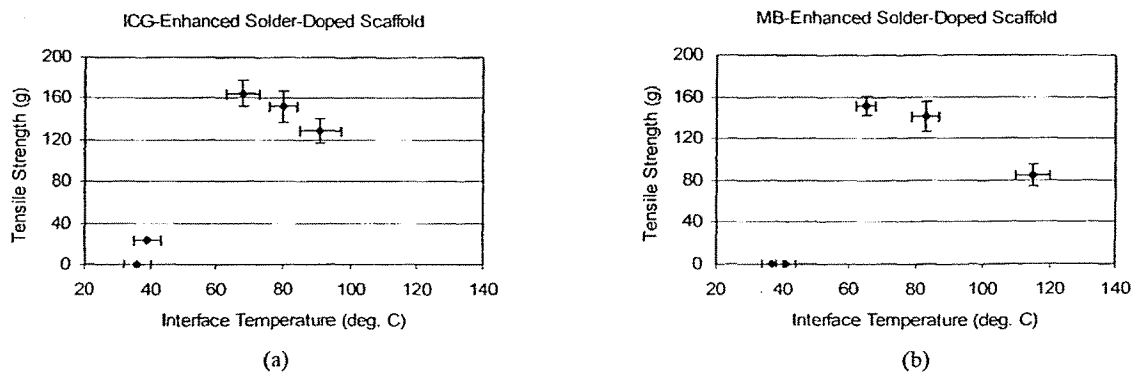


Figure 2: Solder/tissue interface temperature and depth of thermal damage in the tissue substrate expressed as a function of OPD (refer to Figure 1): (a) ICG-enhanced solder used in conjunction with an 808nm diode laser; (b) MB-enhanced solder used in conjunction with a 665nm diode laser; (c) BFC-enhanced solder and (d) GFC (#1)-enhanced solder used in conjunction with a 632.8nm diode laser. [Nb. Lower chromophore concentrations correspond to higher OPD's.] Each point represents the mean and standard deviation for ten repairs.



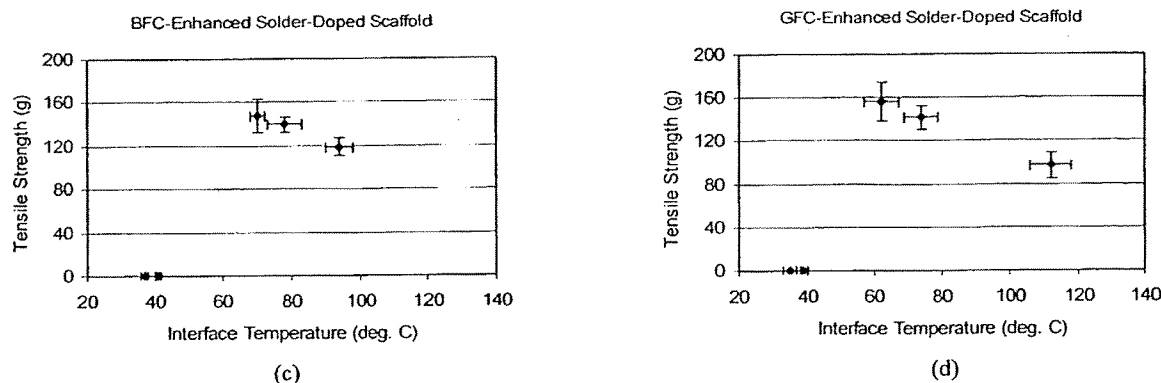


Figure 3: Tensile strength of repairs performed using chromophore-enhanced solder-doped scaffolds as a function of interface temperature: (a) ICG-enhanced solder used in conjunction with an 808nm diode laser; (b) MB-enhanced solder used in conjunction with a 665nm diode laser; (c) BFC-enhanced solder and (d) GFC (#1)-enhanced solder used in conjunction with a 632.8nm diode laser. [Nb. Lower chromophore concentrations correspond to higher OPD's, and subsequently, higher interface temperatures.] Each point represents the mean and standard deviation for ten repairs.

#### 4. DISCUSSION

In a study by Byrd *et al.*, two commonly used chromophores, indocyanine green and methylene blue, were investigated for use in light-activated surgical adhesives, as well as three alternative chromophores: red, blue and green food colorings.<sup>16</sup> Focus on these three alternative chromophores was based on the fact that they all had absorption peaks near the operating wavelength of existing medical lasers. The red food coloring had an absorption peak ( $\lambda = 500$  nm) that would allow it to be used with coumarin dye, Cu Vapor, Ar Ion, and Kr Ion lasers. The blue food coloring absorption peak ( $\lambda = 630$  nm) allows for its use with rhodamine dye, HeNe, Au Vapor, and Kr Ion lasers. The absorption peaks of the green food coloring ( $\lambda = 417$  nm and 630 nm) allow for its use with many different laser systems including a stilbene dye laser, or Kr Ion laser in addition to the lasers mentioned for use with the blue food coloring.<sup>21</sup> Each food coloring investigated demonstrated consistent peak absorption wavelengths when mixed either in deionized water solution or with albumin protein solder.

Another attractive feature of these alternative chromophores is the lack of degradation due to heat and light exposure.<sup>16</sup> ICG and MB, on the other hand, showed a significant decrease in absorbance units with increased time and temperature when heated to temperatures up to 100 °C. Photobleaching was also observed in both ICG and MB solutions with exposure to a white light source. An 88% decrease in absorption was seen in ICG deionized water solution after 7 days of exposure with a corresponding 33% decrease in absorption seen in the MB deionized water solution. Use of these chromophores would cause the protein in the solder to be the limiting factor on the shelf life of the chromophore-enhanced solder-doped scaffolds. The current investigation takes the study completed by Byrd *et al.* one step further with an *in vitro* study conducted to investigate the feasibility of using two of these alternative chromophores for laser-assisted tissue repair in terms of temperature rise at the solder/tissue interface, the extent of thermal damage in the surrounding tissue, and the tensile strength of repairs. RFC was not investigated in this study, due to the lack of availability of a suitable laser source.

Temperature rise at the solder/tissue interface, and consequently the degree of collateral thermal tissue damage, was directly related to the OPD of the laser light in the protein solder. Variation of the chromophore concentration such that the OPD was  $64 \pm 3$   $\mu$ m, corresponding to a little less than half the thickness of the chromophore-enhanced solder-doped scaffold, resulted in uniform results between each group of chromophores, and produced optimal results in terms of minimal thermal damage and maximal tensile strength of repairs. These results are supported by Beer's law, which shows that 85% of laser energy is absorbed within twice the OPD of a material.

At the higher chromophore concentrations investigated (0.75 - 1.0mg/mL ICG or MB and 800 - 1000 $\mu$ L per 13mL BFC or GFC), the laser energy was deposited in the superficial volume of the solder-doped scaffold, resulting in a large accumulation of heat at the surface of the solder before it was conducted to the solder/tissue interface. Heat transfer is proportional to the

temperature gradient across the solder, as described by Fourier's law, and thus, insufficient heat transfer to the vital solder/tissue interface occurred to provide adequate solder-tissue bonding. In fact, repairs formed using these chromophore concentrations were barely strong enough to handle the manipulation required to load them on the material strength testing machine. These results are inconsistent with the results of a previous study conducted by McNally *et al.* where repairs formed using 2.5mg/mL ICG-enhanced solid protein solder in conjunction with an 805nm diode laser produced reasonably strong repairs.<sup>22</sup> The difference between these two studies can be attributed to the fact that the addition of the polymer scaffold acted to reduce the overall OPD of laser light in the solder, hence, reducing heat transfer to the solder/tissue interface. Low chromophore concentrations (0.1 - 0.25mg/mL ICG or MB and 200 - 400 $\mu$ L per 13mL BFC or GFC) with corresponding long OPD's resulted in extensive thermal damage to the underlying tissue and consequently, weaker repairs.

Optimal tensile strength of repairs was achieved by selecting a chromophore concentration that resulted in a temperature of approximately  $66 \pm 3$  °C at the solder/tissue interface. These results are in agreement with initial research conducted by the authors looking at the thermal damage processes that occur in BSA.<sup>22</sup> The study by McNally *et al.* indicated that the threshold temperature for coagulation, as specified by the Arrhenius relation, was approximately 66 °C.<sup>18</sup> Comparable values of threshold temperature have been reported using both spectroscopy and differential scanning calorimetry. Using spectroscopy Arakawa *et al.* determined the thermal denaturation temperature of BSA to be 57 °C.<sup>23</sup> Pico *et al.* determined the denaturation temperature of human serum albumin to be 63.14 °C using differential scanning calorimetry.<sup>24</sup>

## 5. CONCLUSION

The two alternative chromophores investigated in this study, BFC and GFC, produced equivalent results to ICG in terms of collateral thermal tissue damage and optimal tensile strength of repairs when used to enhance solder-doped scaffolds for laser-assisted vascular repairs. In addition, the properties of these alternative chromophores appear to have attractive qualities compared to the commonly used ICG chromophore. The alternative chromophores do not degrade in a deionized water solution or when bound to protein with exposure to ambient light, nor do they degrade with time. These results are encouraging for the improvement of laser-assisted tissue repair techniques. Studies are currently underway investigating an extended range of alternative chromophores for use with light-activated surgical adhesives. Future studies will include exploration of the decomposition products of these chromophores when imbedded in tissue and laser irradiated.

## ACKNOWLEDGMENTS

The authors thank Gary Burgess, Rose-Hulman Institute of Technology, for his assistance in MTS instruction, circuit board design and fabrication, and CNC machining of system components.

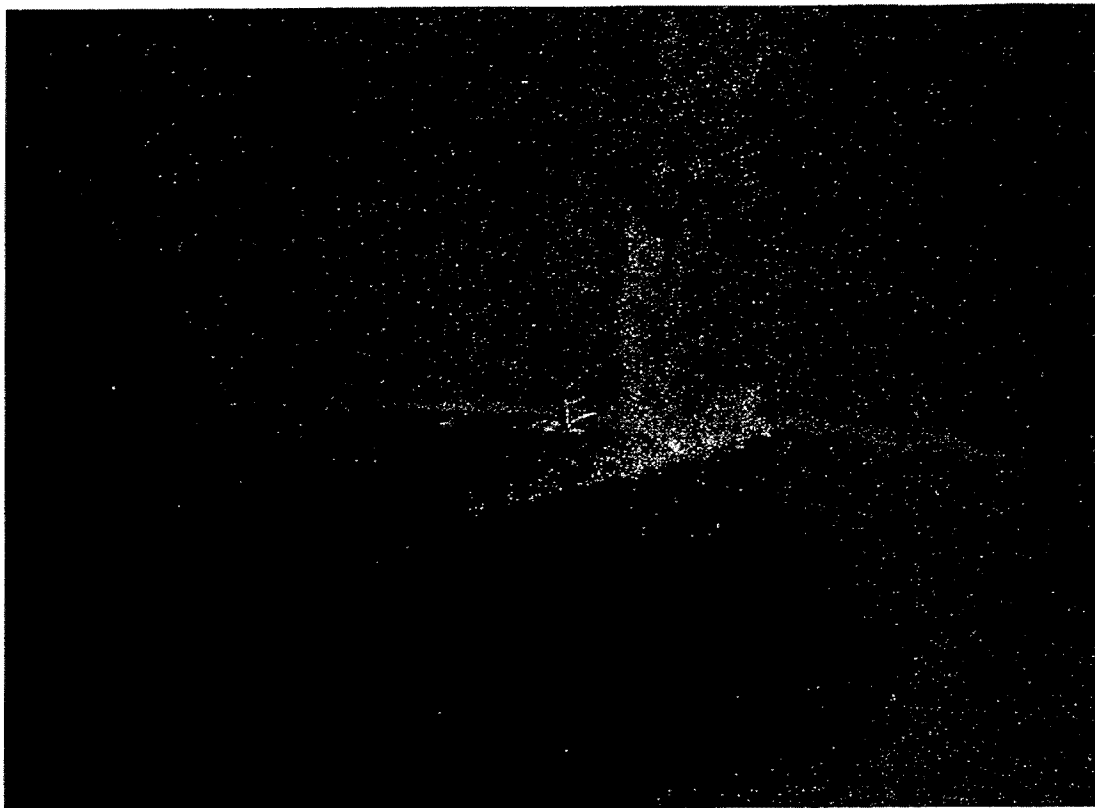
This work was supported in part by Research Corporation through a Cottrell College Science Award, grant CC5010, by Lilly Endowment, Inc. through the Technology and Entrepreneurial Development, grant 960068, made to Rose-Hulman Institute of Technology, and by an Eli Lilly Applied Life Sciences grant.

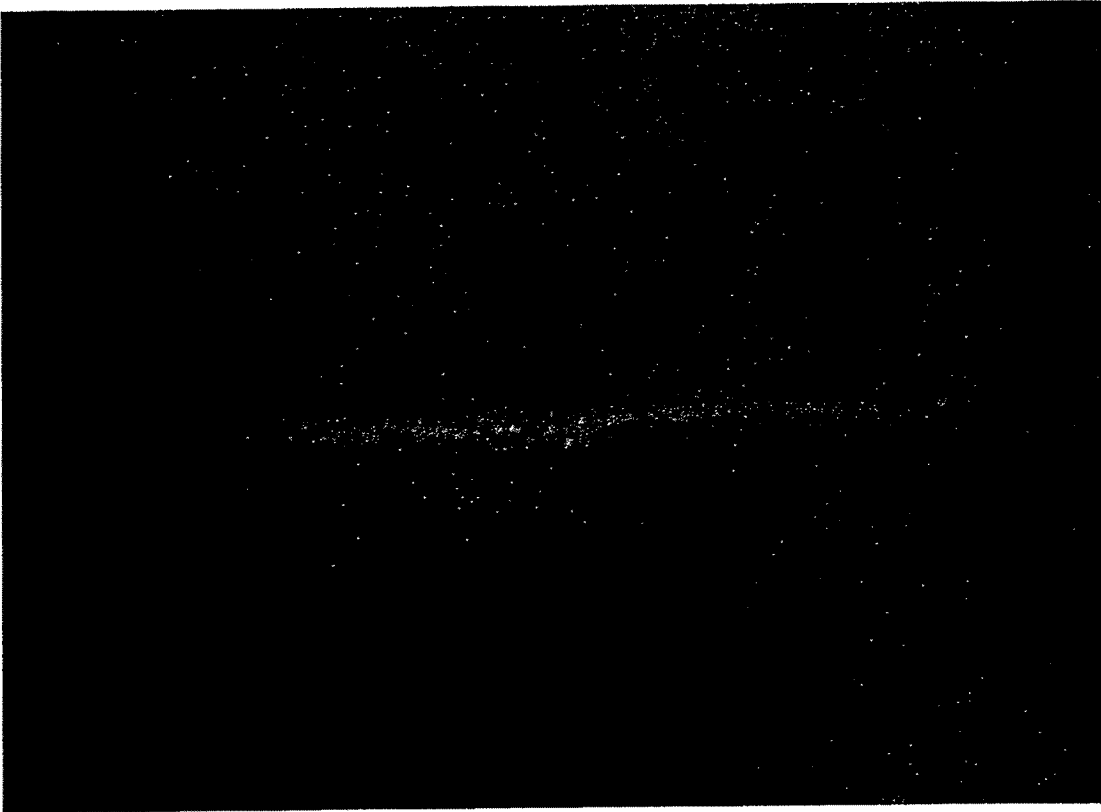
## REFERENCES

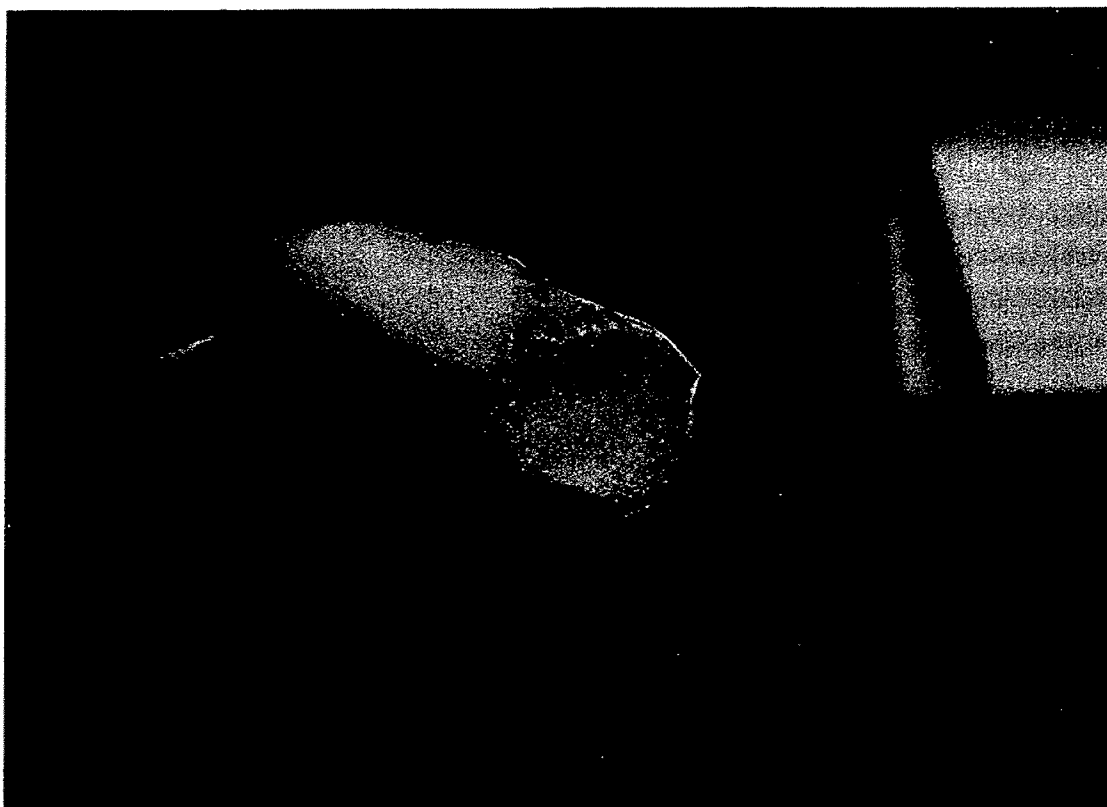
1. Jain KK and Gorish W, "Repair of Small Blood Vessels with the Neodymium-YAG Laser: A Preliminary Report," *Surgery*, **85**(6):684-688, 1979.
2. Krueger RR and Almquist EE, "Argon Laser Coagulation of Blood for the Anastomosis of Small Vessels," *Lasers Surg. Med.*, **5**(1): 55-60, 1985.
3. Poppas DP, Schlossberg SM, Richmond IL, Gilbert DA and Devine CJ, "Laser Welding in Urethral Surgery: Improved Results with a Protein Solder," *J. Urology*, **139**(2):415-417, 1988.
4. Small W, Heredia NJ, Maitland DJ, Eder DC, Celliers PM, Da Silva LB, London RA and Matthews DL, "Experimental and Computational Laser Welding using a Protein Patch," *J. Biomed. Opt.*, **3**(1):96-101, 1998.
5. La Joie EN, Barofsky AD, Gregory KW and Pahl SA "Welding Artificial Biomaterial with a Pulsed Diode Laser and Indocyanine Green Dye," *Proc. SPIE*, **2395**:508-516, 1995.

6. Oz MC, Johnson JP, Parangi S, Chuck RS, Marboe CC, Bass LS, Nowygrod R and Treat MR, "Tissue Soldering by Use of Indocyanine Green Dye-Enhanced Fibrinogen with the Near Infrared Diode Laser," *J. Vasc. Surg.*, **11**:718-725, 1990.
7. Xie H, Shaffer BS, Pahl SA and Gregory KW, "Laser Welding With an Albumin Stent: Experimental Ureteral End-to-End Anastomosis", *Proc. SPIE*, **3907**:215-220, 2000.
8. Kirsch AJ, Cooper CS, Gatti J, Scherz HC, Canning DA, Zderic SA and Snyder HM, "Laser Tissue Soldering for Hypospadias Repair: Results of a Controlled Prospective Clinical Trial", *J. Urol.*, **165**(2):574-577, 2001.
9. Wright EJ and Poppas DP, "Effect of Laser Wavelength and Protein Solder Concentration on Acute Tissue Repair Using Laser Welding: Initial Results in a Canine Ureter Model", *Tech. Urol.*, **3**(3):176-181, 1997.
10. McNally KM, Sorg BS, Chan EK, Welch AJ, Dawes JM and Owen ER, "Optimal Parameters for Laser Tissue Soldering. Part I: Tensile Strength and Scanning Electron Microscopy Analysis," *Lasers Surg. Med.*, **24**(5):319-331, 1999.
11. McNally KM, Sorg BS and Welch AJ, "Novel Solid Protein Solder Designs for Laser-Assisted Tissue Repair." *Lasers Surg. Med.*, **27**(2):147-57, 2000.
12. Mulroy L, Kim J, Wu I, Scharper P, Melki SA, Azar DT, Redmond RW and Kochevar IE, "Photochemical Keratodesmos for Repair of Lamellar Corneal Incisions," *Invest. Ophthalmol. Vis. Sci.*, **41**(11):3335-3340, 2000.
13. Fried NM and Walsh JT, "Laser Skin Welding: In Vivo Tensile Strength and Wound Healing Results," *Lasers Surg. Med.*, **27**(1):55-65, 2000.
14. Kokosa JM, Przjazny A, Bartels KE, Motamedi ME, Hayes DJ, Wallace DB and Frederickson CJ, "Laser-Initiated Decomposition Products of Indocyanine Green (ICG) and Carbon Black Sensitized Biological Tissues," *Proc. SPIE*, **2974**:205-213, 1997.
15. Mikos AG, Thorsen AJ, Czerwonka LA, Bao Y, Winslow DN and Vacanti JP, "Preparation and Characterization of Poly(L-Lactic Acid) Foams," *J. Biomed. Mat. Res.*, **27**(2):183-189, 1993.
16. Byrd BD and McNally-Heintzelman KM, "Alternative Chromophores for Use in Light-Activated Surgical Adhesives," *Proc. SPIE*, 2003 (accepted).
17. Star WM, "Diffusion Theory of Light Transport," in Welch, A.J. and van Gemert, M.J.C., eds., *Optical-Thermal Response of Laser-Irradiated Tissue*, Plenum Press, New York, pp.131-206 (1995).
18. McNally KM, Sorg BS, Bhavaraju NC, Ducros MJ, Welch AJ and Dawes JM, "Optical-Thermal Characterization of Albumin Protein Solders," *App. Opt.*, **38**(31):6661-6672, 1999.
19. Pahl SA, *Light Distribution in Tissue*, Ph.D Dissertation, The University of Texas at Austin, U.S.A. (1988).
20. Glinesky ME, London RA, Zimmerman GB and Jacques SL, "Modeling of Endovascular Patch Welding Using the Computer Program LATIS," *Proc SPIE*, **2623**:349-358, 1995.
21. Katzir A., *Lasers and Optical Fibers in Medicine*, Academic Press, Inc., 1993.
22. McNally KM, Sorg BS, Welch AJ, Dawes JM and Owen ER, "Photothermal Effects of Laser Tissue Soldering," *Phys. Med. Biol.*, **44**:983-1002, 1999.
23. Arakawa T, Hung L, Pan V, Horan TP, Kolvenbach CG and Narhi LO, "Analysis of the Heat-Induced Denaturation of Proteins using Temperature Gradient Gel Electrophoresis," *Anal. Biochem.*, **208**(2):255-259, 1993.
24. Pico G, "Thermodynamic Aspects of the Thermal Stability of Human Serum Albumin," *Biochem. Mol. Biol. Int.*, **36**(5):1017-23, 1995.

EXHIBIT F



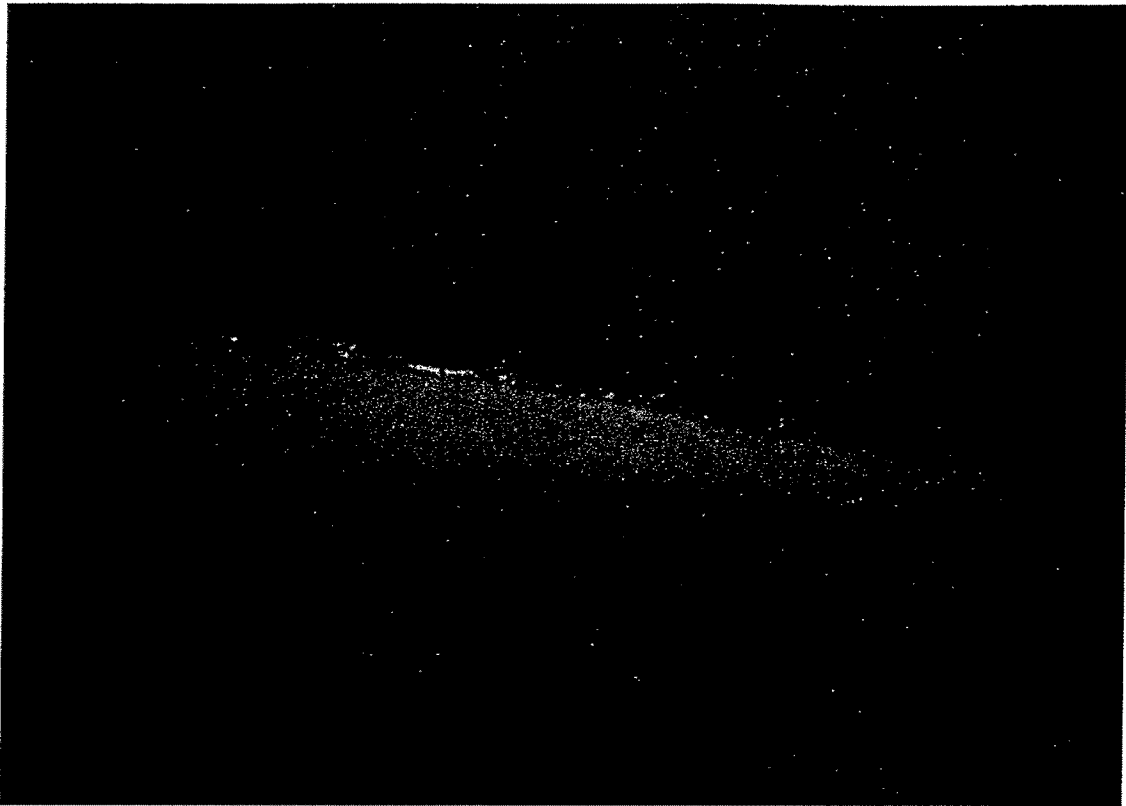




A high-contrast, black and white image of a textured sphere, possibly a planet or moon, set against a dark background with scattered white specks, resembling stars or dust. The sphere is positioned in the upper right quadrant of the frame. It has a grainy, cratered surface with varying shades of gray. The background is predominantly black, with numerous small, bright white dots distributed across it, giving it a cosmic or space-like appearance. The overall image has a grainy, high-contrast quality, similar to a photocopy or a low-quality scan of a photograph.

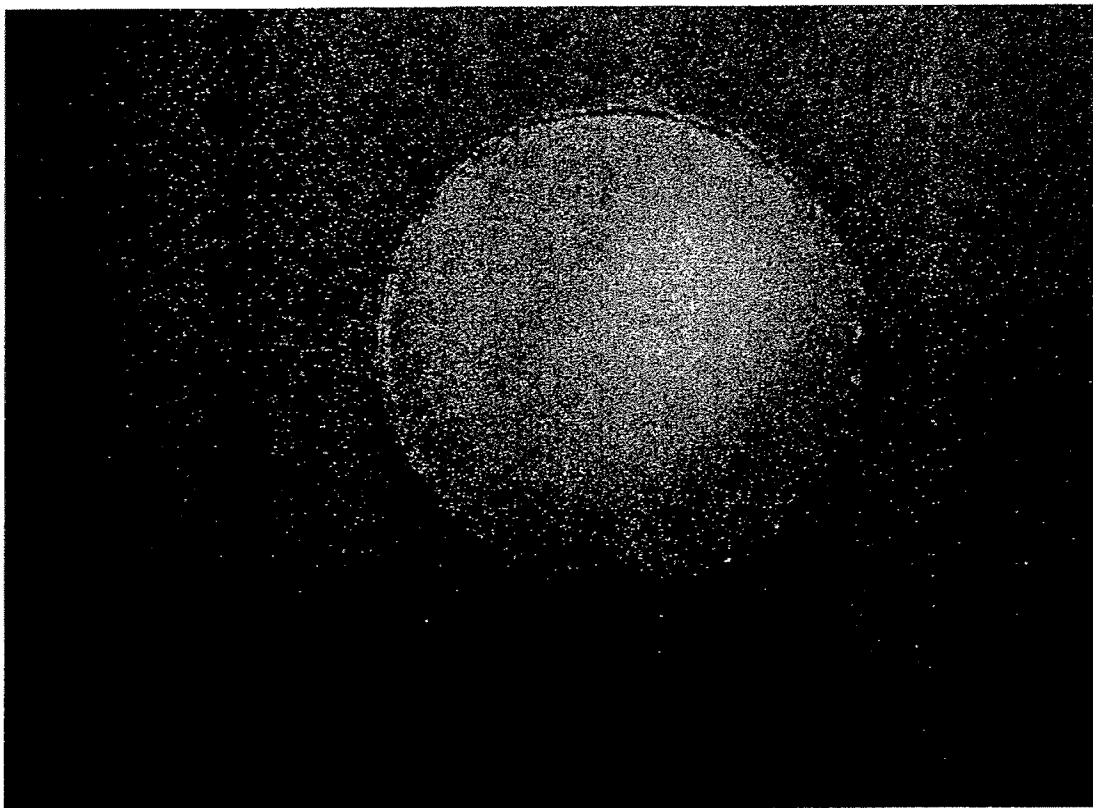
\_\_\_\_\_





This is a high-contrast, black and white image, likely a scan of a physical document. It shows a dark, heavily textured surface, possibly the cover or endpaper of a book. A prominent vertical crease or fold is visible near the center, creating a sharp line of contrast. The texture is grainy and uneven, with many small, light-colored specks and fibers visible against the dark background. The lighting is very dramatic, with deep shadows and bright highlights along the crease and the edges of the texture.

\_\_\_\_\_



# Use of Light-Activated Surgical Adhesive to Join Muscle to Muscle in a Rabbit Model

Rectus extraocular muscles obtained from the Indiana University School of Medicine  
n=40 resulting in n=10 for each of the four groups tested

## Adhesive Parameters:

Group I: 25% BSA (w/v); 0.5mg/ml ICG; 85:15 PLGA; 70% weight fraction NaCl; <106um pore diameter  
Group II: 25% BSA (w/v); 0.5mg/ml ICG; 85:15 PLGA; 70% weight fraction NaCl; 106-150um pore diameter  
Group III: 50% BSA (w/v); 0.5mg/ml ICG; 85:15 PLGA; 70% weight fraction NaCl; <106um pore diameter  
Group IV: 50% BSA (w/v); 0.5mg/ml ICG; 85:15 PLGA; 70% weight fraction NaCl; 106-150um pore diameter  
Adhesive dimensions: 2 x 0.8 x 0.2 mm

Laser Parameters: 805nm diode laser, 1mm spot size, 16 W/cm<sup>2</sup>, irradiation time of 0.5mm/s

Repair Technique: Muscles were harvested approximately 45 minutes after sacrificing the animals. Tissue specimens were stored in phosphate buffered saline for a maximum of four hours before they were prepared for experiments. The approximate length and thickness of each muscle specimen was 8mm and 1.5mm, respectively. A full thickness incision was cut through the tissue specimen width using a scalpel and opposing ends were placed together. Before depositing the solder, the tissue surface was blotted with cotton gauze to remove excess moisture. The adhesive was then denatured with the diode laser. Tensile strength was tested immediately with a MTS tensile testing machine. Specimens kept moist with saline during the procedure to avoid artificially high bond strengths due to tissue drying.

## Breaking Load (g)

Specimen	Group I	Group II	Group III	Group IV	Native
1	256	365	310	371	419
2	237	381	390	582	629
3	262	435	301	480	504
4	275	390	256	464	557
5	240	326	272	432	497
6	253	397	262	422	498
7	256	410	266	477	563
8	230	336	346	358	437
9	227	352	301	378	438
10	275	365	307	368	401
Ave.	251	376	301	433	494
St.Dev.	17	34	42	70	73

## Results of study by Ricci et al., 2000.

	grams	% of native
native	548	
octyl 2-cyanoac suture	94	17.15%
	238	43.43%

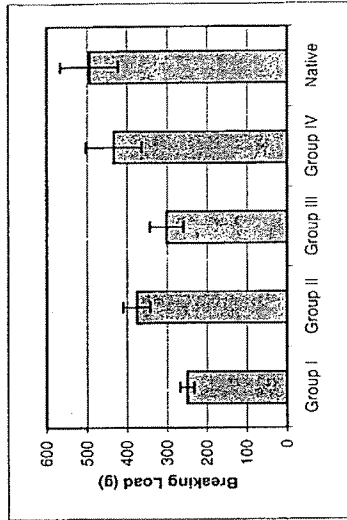


## EXHIBIT G

## Tensile Strength (N) where T=ma

Specimen	Group I	Group II	Group III	Group IV	Native
1	2.5	3.6	3.0	3.6	4.1
2	2.3	3.7	3.8	5.7	6.2
3	2.6	4.3	2.9	4.7	4.9
4	2.7	3.8	2.5	4.5	5.5
5	2.4	3.2	2.7	4.2	4.9
6	2.5	3.9	2.6	4.1	4.9
7	2.5	4.0	2.6	4.7	5.5
8	2.3	3.3	3.4	3.5	4.3
9	2.2	3.4	2.9	3.7	4.3
10	2.7	3.6	3.0	3.6	3.9
Ave.	2.5	3.7	3.0	4.2	4.8
St.Dev.	0.17	0.33	0.41	0.69	0.71

% of native      51%      76%      61%      88%

## EXHIBIT H

Notebook No. \_\_\_\_\_

PROJECT Comparison of LTS upon Smooth vs Rough  
Surface of Membranes

Continued From Page \_\_\_\_\_

Goals

Study conducted to determine if there is any difference in the tensile strength of repairs formed by laying the rough side of the polymer membranes down on the bone vs the smooth side.

Polymer membranes - PLGA (85:15)

- 10wt% NaCl
- manufactured using solvent casting and particulate leaching technique
- cast in 60mm Petri dish

The surface of the membrane in contact with the Petri dish had a smooth surface. The other surface is quite rough. Refer to SEMs from previous studies.

Prior to dealing with proteins, all membranes had a thickness between 0.200 and 0.205mm.

Protein solder : - 50% BSA

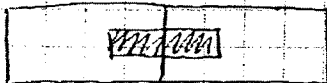
- 0.5mg/ml ICG
- deionized water

- final dimensions  
~ 8 x 4 mm

Membranes left to soak in solder for minimum of 30 mins prior to each procedure.

Laser Parameters :

- 805nm diode laser
- spot size at solder surface = 2cm dia
- $P = 500mW \Rightarrow I = 15.9W/cm^2$
- irradiation time =  $80 \pm 2$  sec



Continued on Page 77

read and Understood By

Signed \_\_\_\_\_

Date \_\_\_\_\_

Tissue preparations refer to notes on page 9 of this lab book.

Strength testing refer to notes on page 10 of this lab book.

### Results:

Rough side of membrane (n=10)

Specimen	Small intestine	liver	kidney	chicken	skin	corrupted artery	artery (chicken)	artery (guinea pig)
1	96	142	101	87	168	104	151	138
2	90	128	97	84	143	92	147	143
3	94	115	90	90	155	98	160	138
4	102	123	92	82	159	110	156	145
5	117	134	111	85	163	96	139	150
6	97	119	107	81	168	115	164	144
7	88	130	85	88	152	118	171	151
8	91	126	104	93	147	107	157	146
9	94	120	98	89	164	105	151	141
10	86	126	102	90	172	111	159	137
Mean	96	126	99	87	159	106	156	143
SD	9	8	8	4	10	8	9	5

Compare these results with previous study (starting page 9 of this lab book):

Mean	94	136	98	90	152	101	151	140
SD	9	10	6	8	7	8	11	6
n	7	8	8	6	7	5	7	6

[Nb: we had attempted to use rough side of membranes in this previous study, however, this was not verified in all cases prior to placing the adhesive on the tissue.]

Continued on Page 78

Read and Understood By

Signed

Date

PROJECT Comparison of LIS using smooth vs rough  
surfaces of membranes

NOTEBOOK NO. \_\_\_\_\_

Continued From Page \_\_\_\_\_

Students t-test:

$$t = \frac{\bar{x}_1 - \bar{x}_2}{\sqrt{\frac{s_1^2}{n_1} + \frac{s_2^2}{n_2}}}$$

$$df = (n_1 + n_2 - 2)$$

$$\alpha = 0.05$$

	Small intestine	liver	kidney	spleen	oleum	coronary artery	aorta (intima)	aorta (adventitia)
t	0.34	2.25	0.21	0.89	1.76	1.03	0.39	1.14
%	0.5	0.02	0.8	0.2	0.05	0.2	0.2	0.2
df	15	16	16	14	15	13	15	14

no significant difference in any of the tissue types tested in this study and previous study (starting pg. 9 of this lab book)

Smooth side of membrane (n=10)

Specimen	Small intestine	liver	kidney	spleen	oleum	coronary artery	aorta (intima)	aorta (adventitia)
1	86	119	85	72	136	107	132	111
2	74	122	93	66	142	102	146	122
3	93	114	85	69	130	110	128	120
4	81	118	81	75	135	95	135	134
5	77	106	80	77	133	92	142	127
6	85	110	74	70	137	90	122	125
7	90	115	87	72	151	97	125	121
8	71	118	85	65	138	103	131	117
9	69	109	88	68	129	101	139	132
10	83	111	97	63	144	99	120	121
Mean	81	114	86	70	138	100	132	123
SD	8	5	7	4	7	6	9	7

Comparison of data using rough side vs smooth side of membranes:

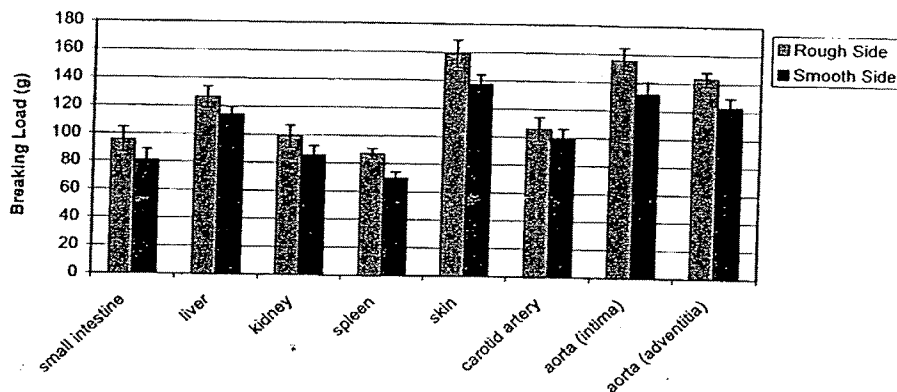
	Small intestine	liver	kidney	spleen	oleum	coronary artery	aorta (intima)	aorta (adventitia)
t	3.86	4.08	4.05	9.28	5.82	1.81	5.97	7.64
%	0.001	0.0001	0.0001	0	0.00001	0.05	0.00001	0
df	18	18	18	18	18	18	Continued on Page 18	

Understood By \_\_\_\_\_

Signed \_\_\_\_\_

Date \_\_\_\_\_

\* The strength of the repairs were found to be significantly better (Student's t-test with  $\alpha = 0.05$ ) when using the rough side of the membrane compared to the smooth side of the membrane for all tissue types except for the carotid artery.



\* Pinholes remained relatively small for both rough and smooth sides of membranes.

Continued on Page \_\_\_\_\_

Read and Understood By \_\_\_\_\_

Signed \_\_\_\_\_

Date \_\_\_\_\_